ADDIS ABABA UNIVERSITY

ADDIS ABABA INSTITUTE OF TECHNOLOGY

SCHOOL OF MECHANICAL AND INDUSTRIAL ENGINEERING

ANALYSIS OF AERODYNAMIC BRAKES IN MAINLINE OF ETHIOPIA RAILWAY CORPORATION (**ERC**)

ANALYSIS OF AERODYNAMIC BRAKES IN MAINLINE OF ETHIOPIA RAILWAY CORPORATION (ERC) 2015

A Thesis submitted to the School of Graduate Studies of Addis Ababa University in partial fulfillment of the requirements for the Degree of Masters of Science in Mechanical Engineering (Railway stream)

By: Hillina Admasu

Advisor:- Tsegaye Feleke

March 2015

ADDIS ABABA UNIVERSITY

Addis Ababa Institute of Technology

School of Mechanical and Industrial Engineering

(Stream: Mechanical Railway Engineering)

Master's Program Final Thesis Acceptance Approval Form

Thesis Topic: Analysis of aerodynamic brakes in mainline of Ethiopia Railway Corporation (ERC)

By: **Hillina Admasu**

Approved By Board Of Examiners:

Mr. Tsegaye Feleke Advisor	_____ Signature	_____ Date
Mr. Habtamu Tkubet Internal Examiner	_____ Signature	_____ Date
Mr, Yidnekachew External Examiner	_____ Signature	_____ Date
Dr. Birhanu Beshah Railway Head Center	_____ Signature	_____ Date

TABLE OF CONTENTS

ABSTRACT

Aerodynamic brakes are used as auxiliary braking system in rolling stock. The aerodynamic brake is defined as a stiffened plate subjected to lateral pressure load considering buckling behavior. This research is prepared for the computational fluid analysis (CFD) of aerodynamic braking plate by using Finite Element Method to improve arrangement of braking plate and analyze for Ethiopian National Train (ENT).Through the research the current speed of ENT IS taken(120km/hr) and also assumed future speed of 300km/hr is also considered.

The analysis is done using the parameters of the rolling stock to be used by Ethiopian Railway Corporation. The assembly of the train body and braking plate area was modeled by using CATIA software. After modeling, analysis for determination of brake force is used by ANSYS Fluent and also the amount of pressure is discussed under four main cases. When the braking plates are positioned at four different angles (45^0, $60^{0,}$ $75^{0,}$ & 90^0).The results showed that the drag coefficient increases as the speed increases and also at 120km/hr the aerodynamic effect is less than at 300km/hr.

At 120km/hr all the results of pitch moment coefficient were less than one this shows that the train is stable under all four cases. The drag force at an arrangement of 90^0 was found to be enough to slow down the train at a deceleration of $0.68m/s^2$ .All the other three cases were invalid because the system cannot achieve the required deceleration. The analysis when the two trains cross each other both equipped with aerodynamic braking plate was also analyzed. The result achieved was the maximum pressure during crossing was 2.39kpa.this pressure can be easily resisted by the window glass which can resist 8.3kpa pressure. Therefore the system can work without any pressure effect. The results were discussed by displaying the drag coefficient, the lift coefficient, residuals, moment coefficient and pressure

Key words: *CFD, aerodynamic drag, shape optimization, cross wind stability, Fluent, Inflation*

ACKNOWLEDGMENT

I wish to express my genuine appreciation to my advisor Mr. Tsegaye Feleke for his unlimited support, direction, advice, and patience with me during the research preparation. I would like to extend my special thanks to all my families and friends for their kind help and cooperation in various ways during this thesis work.

List of tables

List of figures

Nomenclature

A Area

C_f Coefficient of friction along wall

C_l Coefficient of Lift

C_d Coefficient of Drag

C_p Coefficient of Pressure

D Drag force

g Gravity

$K-Epsilon$-Turbulence model to simulate and read turbulent flow

M Mach number

P Pressure

Re Reynolds number

Re_x Reynolds number along a position x

U_{cl} Centerline Velocity

u_∞ Fluid velocity

u Friction velocity

U_{max} Max. Velocity

V Velocity

V_{inlet} Inlet Velocity

y_p Distance to the wall from center of pipe

y^+ Non-dimensionalized distance of first grid point from wall

ρ Density

τ Shear Stress

μ Dynamic viscosity

$\dot{Q_{net\,in}}$ Rate of input energy

$\dot{W_{net\,in}}$ Rate input work

HST High Speed Train

RT Regional Type

ERC Ethiopian Railway Corporation

ENT Ethiopian National Train

AA-DD Addis Ababa-Dire Dawa

ETSC European Transport Safety Council

UIC International Union of Railways

CFD Computational Fluid Dynamics

LES Large Eddy Simulations

CAD Computer Aided Design

R Residual

N Number of iteration

F_x Aerodynamic drag

F_{px} Pressure Drag

$F_{\tau x}$ Friction drag

F_R Total drag

a, b, c Constants determined by the experiment

F_t Train velocity relative to the ground

q Dynamic pressure

s_x Cross-sectional area of the train

c_x Coefficient of aerodynamic drag

F_{xt} Drag of the leading car or locomotive

F_{xw} Drag of the tail car

F_{xz} Friction along the train

n Number of middle carriage

c_{xt} Drag coefficient of the leading car or locomotive

c_{xw} Drag of the tail car

c_{xz} Friction coefficient along the train

p_{bx} Skin pressure of the train along x axis

s_F Area of the train wall surface

τ_{ix} Shear stress on the train along x-axis

μ Viscosity of the air

RANS Reynolds-Averaged Navier-Stokes

EIV Expected Improvement Value

MDO Multidisciplinary Optimization

RSA Response surface approximation

α Yaw angle

l_1 Length of upper curve

l_2 Length of the lower curve

c_1 Upper nose curve

h Height of the nose

c_2 Lower nose cure

dl_1 Change in length of upper curve

dl_2 Change in lower curve length

dh Change in nose height

DOE Design of experiment

FCCD Faced Centered Composite Design

$y_{c,new}$ Y-coordinate of the curve after the deformation,

$y_{c,old}$ Y-coordinate of the curve before deformation

i Coordinate point

n_c Number of coordinate points

L Length

H Height

W Width

CCD Center Composite Design

N Number of Design Variables

dy_{c1} Deformation coefficient c_1

dy_{c2} Deformation coefficient c_2

a Mechanical resistance

b Non-aerodynamic coefficient

b_1 Loss of quantity during the motion

b_2 Resistances caused by loss of gearing

c Aerodynamic drag term constant

k_w Relative velocity coefficient

k_y Change penetration coefficient

k_t Tunnel effect coefficient

r Specific aerodynamic drag

i Specific gradient resistance

r_c Specific curve resistance

R Total mechanical and aerodynamic drag

m Train mass

c_x Frontal aerodynamic coefficient

c_y Lateral aerodynamic coefficient

c_p Pressure coefficient

F_x The total effective force

ΔS Change in distance

L_o Mechanical labor

$\bar{u}$ Average fluid speed

F_o Locomotive traction force

l_i Indicated mechanical labor

H_i lowest caloric value of the diesel fuel

dC_D Elementary fuel consumption

η_1 Output/turnover of the locomotive

f_f Friction factor

CHAPTER ONE

1. Introduction

1.1. Background

1.1.1. World History of rolling stock

Rolling stock used on railways in the earliest days evolved from carriage and wagons which ran on highways to carry people and bulk materials. As early as the sixteenth century, wooden wheeled carts were used in mine and quarries running on longitudinal timber rails. With the progressive evolution of the skills and crafts of the wheelwright metalworker and the iron-maker, wheels improved through various phase from simple rough turned wooden spools through spoked and rimmed construction to fully cast and turned metal wheels. Similarly, body construction and springing, particularly for passenger carrying vehicles, relied very heavily on the experience gained in the construction of stagecoaches in the seventeenth and eighteenth centuries.

At the end of the eighteenth century, horse drawn trams running on metal rails began to appear in a number of European cities. These horse drawn tramways were literally to pave the way for development of railways when steam power began to be developed early in the 1800's. One has only to look at illustrations of early passenger coaches to see how closely they resemble the road vehicles of the previous century. As railway experience was gained, the design of rolling stock also evolved. Springing, body structure, wheels and axles all are subject to varying loads and stresses, when comparing slower speeds on rough roads to much faster speeds on railways, with a comparatively smoother ride.

Railway rolling stock generally runs on hard wheels on hard rails. The wheels are not only supported by the rails but are guided by them. The only exception to this is for a small number of metros where rubber tires have been introduced. In this case the supporting function of the rail may be separated from the guiding function. In all cases, railway rolling stock will transmit vertical, horizontal and longitudinal forces to the track and its supports. Most railways have adopted twin rails and flanged wheels. Forces are transmitted to the rail structure either by

direct bearing on the rail top from the wheel tire, or by bearing laterally through the flange, or by longitudinal friction. Potential 'overturning' forces caused by centrifugal force on curves, coupled with wind forces on exposed locations are resisted by vertical dead weight and super-elevation or 'cant' on curves. Railway network in the world has about 1.2 million km total length of which about 1.93 million km on normal track (1435 mm), (European normal gauge central network ca. 195 000 km) 0.2 million km narrow gauge (<1435mm) 0.25 million km broad gauge On these networks following vehicles type are riding: 86 000 diesel locomotives, 27 000 electric locomotives, 3.8 million freight cars and 180,000 passenger cars. [1]

1.1.2. History of Ethiopian railway

Discussion of an Ethiopian railway was initiated by Alfred Ilg, an advisor to Emperor MenelekII. He had attempted to interest the previous emperor and other Ethiopian political figures in the construction of a railway to replace the six-week mule trek between the capital and the French port city, but had no success. When Menelek acceded to the throne in 1889, negotiations began a new and a decree was granted on February 11, 1893, to study the construction of rail line. Ilg, a Swiss citizen, and a number of French associates put together a firm and received a royal charter on March 9, 1894, enabling them to start work. Menelek resisted personally putting any funds into the venture, but did grant a 99-year lease to Ilg and his associates in return for a number of shares in the firm and half of all profits in excess of 3,000,000 francs. Furthermore, the firm was obliged to construct a telegraph line along the route.

A group of British investors calling themselves the New Africa Company effectively took control of the firm over several years. They provided a new source of capital and by 1901 had joined with the French investors to form the International Ethiopian Railway Trust and Construction Company - a holding firm which essentially controlled the railway and supplied it with further capital. The first commercial service began in July 1901, from Djibouti to DireDawa.

Ethiopia's share in the railway was seized by the Italian government in the Second Italo-Abyssinian War, but was regained by Ethiopia after the World War II. Following the

independence of Djibouti in 1977, the French share in the railway was transferred to the new nation.

The railway company carried out surveys for extending its line 310 kilometers south from Adama to Dilla between 1960 and 1963. The government formed a Nazareth-Dilla Railway Development Corporation to support this new branch. Although the French government offered a loan to fund this new branch in 1965, and Yugoslav experts had studied and thought the project would be worthwhile, this project was never carried out.[2]

In 2003 the European Commission prepared a grant of EUR 40 million for the rehabilitation of the Djibouti-Ethiopia Railway. Reflecting increases in fuel and steel prices, the commission increased this grant to EUR 50m in 2006. The Djiboutian Ministry of Equipment and Transport and the Ethiopian Ministry of Transportation and Communications chose the South African firm Comazar to administer the railway in March 2006. A 25-year concession was due to be signed in June 2007, but this failed to happen, and negotiations began with Kuwaiti company Fouad Alghanim and Sons Group.

In January 2010, it was announced that the Ethiopian government had signed a memorandum of understanding with four companies to build a new rail network. Among these firms was the China Communications Construction, China Railway Group, and an Indian and Russian company. After all parties except the Chinese firms failed to take further action; the contract was awarded to the CRCG. In August, funding for the project was agreed to come from the Export and Import Bank of China. In September 2010, construction began on the project.

The network will be 5,000 km long, and radiate from Addis Ababa. It will be constructed in two phases, the first phase involving the construction of five lines. The project will provide 300,000 jobs in construction and cost $336 million annually for five years. The system will handle 6 million tons of freight. The government of India has given US$300m for the Mekelle-Djibouti rail line.

The gauge of the new railway will be 1,435 mm (4 ft 8 $\frac{1}{2}$ in), which is standard gauge, as there is no point in increasing the size of the network fourfold on an obsolete gauge. There are also standard gauge proposed changes in adjacent countries, besides connecting with this

gauge in northern Africa, the Middle East, Europe and China, among other areas. Also included was a light rail system in Addis Ababa.[3]

1.1.3. Rail vehicle

The principal difference between railway vehicle and other types of wheeled transport is the guidance provided by the track. The surface of the rails not only supports the wheels, but also guides them in a lateral direction. The rails and the switches change the rolling direction of wheels and thus determine the travelling direction of the railway vehicle. The running gear is the system that provides safe motion of the vehicle along railway track. The running gear includes such components as wheel sets with axle boxes, the elastic suspension, the brakes, the traction drive, and the device to transmit traction and braking forces to the car body .Its main functions are Transmission and equalization of the vertical load from the wheels of the vehicle to the rails, Guidance of vehicle along the track, Control of the dynamic forces due to motion over track irregularities in curves, switches and after impacts between the cars efficient damping of excited oscillations application of traction and braking forces.

Depending on the running gear, the vehicles may be described as boogied or bogie-less. In vehicles without bogies the suspension, brakes, and traction equipment are mounted on the car body frame. The traction and braking forces are transmitted through traction rods or axle box guides (sometimes known as "horn guides"). Conventional two-axle vehicles will generate larger forces in tight curves than the equivalent bogie vehicle; therefore their length is limited. Running gear mounted on a separate frame that can turn relative to the vehicle body is known as a bogie (or truck). The number of wheel sets that they unite classifies the bogies. The most common type is the two-axle bogie, but three- and four-axle bogies are also encountered on locomotives. Previously, the bogies simple yallowed the running gear to turn in a horizontal plane relative to the car body thus making it possible for the wheel sets to have smaller angles of attack in curves. In modern bogies, the bogie frame transmits all the longitudinal, lateral, and vertical forces between the car body and the wheel sets.

The frame also carries braking equipment, traction drive, suspension, and dampers. It may also house tilting devices, lubrication devices for wheel-rail contact and mechanisms to provide radial positioning of wheel sets in curves. Boogied vehicles are normally heavier than two-axle

vehicles. However, the design of railway vehicles with bogies is often simpler than for two-axle vehicles and this may provide reliability and maintenance benefits.

1.1.4. Train braking

Train braking is a very complex process, specific to rail vehicles and of great importance by the essential contribution on the safety of the traffic. This complexity results from the fact that during braking occur numerous phenomena of different kinds - mechanical, thermal, pneumatic, electrical, etc. The actions of these processes take place in various points of the vehicles and act on different parts of the train, with varying intensities. The major problem is that all must favorably interact for the intended scope, to provide efficient, correct and safe braking actions.

The purpose of braking action is to perform controlled reduction in velocity of the train, either to reach a certain lower speed or to stop to a fixed point. In general terms, this happens by converting the kinetic energy of the train and the potential one - in case of circulation on slopes - into mechanical work of braking forces which usually turns into heat, which dissipates into the environment.

At first, the rather low locomotives power and traction force allowed braking using quite simple handbrakes that equipped locomotives and eventually other vehicles of the train. As the development of rail transport and according to increasing traffic speeds, tonnages and length of trains, it was found that braking has to be centralized, operated from a single location - usually the locomotive driver's cabin and commands have to be correctly transmitted along the entire length of the train.

As a consequence, along the time, for railway vehicles have been developed various brake systems, whose construction, design and operation depend on many factors such as running speed, axle load, type, construction and technical characteristics of vehicles, traffic conditions, etc.

Among various principles and constructive solutions that were developed, following the studies and especially the results of numerous tests, the indirect compressed air brake system proved to

have the most important advantages. Therefore, it was generalized and remains even nowadays the basic and compulsory system for rail vehicles. It is still to notice that, regarding the classical systems used for railway vehicles, there are also several major challenges that may affect the braking capacity. These aspects must be very well known and understood, so as to find appropriate solutions in such a manner that the problems to be overcome by applying different constructive, functional, operational and other kinds of measures.

For example, one of these issues is the basic braking systems dependency on the adhesion between wheel and rail, which can lead to wheel blocking during braking. This determines not only the lengthen of the stopping distance, but also the development of flat places on the rolling surface of wheels, generating strong shocks transmitted to the rail and to the vehicle, with damage to traffic safety and comfort of passengers or goods transported integrity. This has generated particular concerns regarding the design and implementation of more efficient wheel slip prevention devices capable to avoid the above-mentioned phenomena with as small as possible reduction of braking capacity.

Another major problem is the friction between wheel and brake shoes, brake pads and disc respectively, which leads to severe thermal regimes and special thermal fatigue nature efforts, requiring specific constructive and operating standards. More than that, due to the air compressibility and to the length of trains, the pneumatic commands propagates with limited speed in the brake pipe and, as a result, there always is a delay in the braking of neighboring vehicles. As a consequence, the rear vehicles are running into the front ones, producing large dynamic longitudinal reactions in buffers and couplers. The induced compression and tensile forces can reach significant levels, affecting both the rolling stock and the track, even conducting to deteriorations of safety operation of the trains.

Railway high speed operations also determined more severe requirements for braking systems, given to the necessity to develop higher braking forces and to dissipate larger amounts of energy in a short time, not to mention the problem of wear in the case friction brakes. In that case, complementary systems whose performance and reliability are safety relevant were developed to enhance the braking capacity. These several issues, even briefly presented, reveal not only the importance and complexity of braking systems used for rail vehicles, but also the

necessity of knowledge and understanding the problems in order to develop equipments increasingly more efficient and reliable.

Generally the complementary braking systems provide consistent controllable braking forces permitting speed reductions but, unlike the basic ones, the braking efficiency decreases at low running speeds. As a consequence, there have to be used together with a basic braking system to ensure the capability of stopping at fixed point and of maintaining the vehicle standstill on slopes.

Complementary braking systems add braking power without having the thermal capacity limitations of the friction wheel or disc brakes that would necessitate expensive solutions or lead to excessive wear from harder use. More than that, those which are independent of wheel/rail adhesion improve safety by enabling shorter stopping distances when applied by giving a reduced dependency between stopping distance and adverse adhesion conditions caused by moisture, ice, leaves or other pollution on the top of the rails, etc.

That is why usually the decision to equip rail vehicles with complementary braking systems relies either on the incapacity of basic wheel-rail adhesion dependent brakes to ensure the braking necessary capacity for high speed trains and, in that case, there are necessary adhesion independent braking systems, or to diminish the wear of the friction based braking systems, in that case being useful the dynamic braking systems.

The complementary braking systems used are the magnetic rail brake, eddy current brake, dynamic braking, regenerative braking, and air resistance (aerodynamic braking). In this paper aerodynamic braking will be discussed.[4]

1.1.5. Aerodynamic braking

In general, aerodynamic brakes have been used in the domain of aircraft and flight constructions as well as for high-speed trains. Aerodynamic problems linked with high-speed train systems are nowadays receiving a considerable attention as practical engineering problems. With train speed increase, many engineering problems, which have been reasonably neglected at low speeds, are being raised with regard to aerodynamic noise and vibrations,

impulse forces occurring as two trains intersect each other, impulse wave at the exit of tunnel, ear discomfort of passengers inside the train, etc. These are some of major limiting factors to the increase of train system speed. Such aerodynamic problems are closely associated with the flows occurring around railway trains.

Besides conventional brakes, high-speed trains also use aerodynamic brakes as additional braking systems. Aerodynamic brakes are designed to generate a braking force by increasing a drag by pulling the panels on the car roof, thus increasing the surface area exposed to the incoming air stream.

When the aerodynamic brake is in the extended position, it blocks the airflow and overpressure occurs in front of it, while behind it an area of negative pressure is formed due to the flow separation behind the plate. The difference in pressures between the front and the rear brake panel surface creates a resistance force normal to the surface of the panel and serves as a braking force. The tangential force induced by the surface friction is negligible when compared to the normal force.[5]

An aerodynamic train drag increases with the square of speed, and an aerodynamic brake system has a very good performance, particularly at high speeds. Therefore, aerodynamic brakes are classified as high speed brakes. It is very interesting to determine their effectiveness when a train reaches speeds higher than 100 m/s. An aerodynamic brake is considered as a stiffened aluminum plate. Stiffened plates are basic building elements in many civil as well as aircraft structural applications and, as such, accurate strength assessment of individual stiffened plate components is one of the key parameters to perform a general strength analysis. These structural components typically consist of a plate with equally spaced stiffeners (flat bar or T- and L- sections welded on one side) and often with intermediate transverse stiffeners, frames or bulkheads.[6]

1.2. Statements of the problem

Most of railway vehicles are using disc brakes for braking. The main problem of braking and stopping a heavy railway vehicle is great heat load into brake disc in a very short time. An overview of past research showed that brake discs for rail vehicles are mostly tested on thermal loads and their effects. Long repetitive braking leads to temperature rise of various components of vehicle brake system that reduce the performance of braking.

High temperatures during braking may cause:

- ✓ premature wear
- ✓ bearing failure
- ✓ thermal cracks and
- ✓ thermal excited vibration

In order to avoid this auxiliary braking systems are used. One of the breaking systems is aerodynamic braking system .By using this braking system the speed of the rolling stock is lowered before engaging in main braking system.

In the Ethiopian national train (ENT) which is from Sebeta to Djibouti the train stops at the substations and main stations decelerating from a speed of 120 km/hr. Due to this there exists high energy dissipation causing the above listed problems. This paper will address them by designing and analyzing aerodynamic brake that can perform the heat dissipation at a speed of 120km/hr.

In addition to this, if ERC is going to use a high speed train in the future with a speed of reaching 300km/hr, analyzing this situation using aerodynamic brake so that appropriate recommendation will be generated accordingly.

1.3. Objective of the study

1.3.1. General objective

The general objective of this research is to determine the braking plate area for the mainline from Sebeta to Djibouti and perform the computational fluid dynamics (CFD) analysis using the technical parameters of locomotives of ERC.

1.3.2. Specific objective

Specifically this research is aimed in:

- Determine the brake plate area
- CFD analysis of the Aerodynamic brake
- Discuss the results of the analysis
- Make conclusion and recommendation based on the results from the analysis

1.4. Scope of the study

This paper includes determination of aerodynamic brake plate area and analysis on the brakes by using the current parameters of the main line (from Sebeta to Dijubuti). The software ANSYS Fluent is used to perform the analysis.

1.5. Limitation of the study

The limitations during this research are lack of data because the operation of the train is not yet in process. Some data are to be taken from other countries that have been practicing same type of transportation. This paper does not include the manufacturing of the aerodynamic brake system components. Experimental analysis will not also be considered in this paper.

1.6. Research methodology

This paper will use qualitative and quantitative data analysis technique, and Finite element (FE) method is used to assess structural behavior of the aerodynamic brake installed for the mainline using ANSYS software. A lot of paper and journal has been read up and a part of it has been considered in this project. Meanwhile, the actual vehicle body dimension has been taken from ERC specification for analysis purpose.

There are two levels in the virtual prototype study. First in the development of various functional modules software such as pro-E, solid work CATIA, UG, CAXA, etc .For this research CATIA will be used for 3d modeling. The second one is analysis software. There is a lot of structural software (i.e. ADAMS/RAIL, SIMPACK, NUCARS, VAMPIER, DADS/RAIL, ANSYS) and ABACUS .For this research will be use ANSYS, or/and SIMPACK software

CHAPTER TWO

2. LITERATURE REVIEW

During this research there has been a lot of researches read, the following reviewed articles are the most related to the title and works to be done. Each research had all different methods included and also from different perspectives but each point raises necessary information on the design and analysis of aerodynamic brakes on trains.

Slavica Ristic, this research is done with the title "determination of braking force on the aerodynamic brake by numerical simulation" the train consists of two locomotives at each end and four passenger cars between, with 121m of overall length. The analysis is done by using three speeds (30m/s, 50m/s and 70m/s). Slavica used three plates arranged in a way that the distance between the first and the second plate was 17m and between the second and the third was 20m.This research mainly dealt with the relationship of the distance between the plates with the drag force. The method used was numerical simulation using ANSYS Fluent12.1.The results from this simulation were for train without aerodynamic brake and the train with one, two and three aerodynamic brakes over the train roof.

He showed that low-pressure zones were arising behind the panel and the high -pressure zone in front of the panel, resulted from the creation of the drag force on the brake. For all the three brakes, dimensions of the intensive vortex "bubble", behind the panel, was analyzed. Salvica noticed that the "bubble" length at the first and third brake is the same, while the "bubble" behind the second brake has shorter length. This was caused by the fact that the distance between the first and second brake was smaller than distance between the second and third one. A dimension of the "bubble" depends also of train velocity. The "bubble" was largest when the train velocity was highest (by 70m/s).It was also showed that braking panels, placed at the first position, were creating the largest drag, while for panels at the second and other positions drag force is decreasing, and that means their contribution to the braking force is low.

At the first brake the separation of air streamlines was occurring so the second brake was implicated by vortex trail of the first brake. Contributions to the braking force of every single

brake, obtained by FLUENT simulations and those from pressure distributions in front and behind the panel, showed good correlation of results with the aerodynamic drag calculations for flat plate, disposed orthogonally to the flow stream. Contributions of every brake to the gross braking force of observed train, were as follows for the first brake it was 24%, for the second 15% and for the third one 14.8%. These results were in correspondence with the results from tests made for the train Maglev on the Yamanashi test railway. The future works to follow this research were to determine the relationship between the drag force and each of the following parameters: flow of speed, brakes geometrical shape and angle of attack.[13]

Ivana Vasović, Mirko Maksimović, Mirjana Puharić,Dušan Matić and Suzana Linić1: the title of the research is "structural analysis of aerodynamic brakes in high-speed trains". The geometry of the train analyzed was the same as the Slavica's research. In their research the main focus was structural analysis of aerodynamic brake. The work consisted of two parts; Part I deals with the aerodynamic load distribution of train brakes, and Part II treats stiffened panels surrounded by strong support members such as longitudinal girders and transverse frames. The material used for the construction of aerodynamic plate was stiffened aluminum AA6082-T6. The researchers used commercially available finite element code NASTRAN was used for the stress analysis. Both the plate and the stiffeners are modeled using shell finite elements selected from the NASTRAN library of elements and were subjected to lateral pressure loads. In order to obtain the minimum weight of the structure, the initial dimensions of the train brake are reduced in steps to satisfy allowable stresses of aluminum material and buckling load behavior. At the end the thickness of the rib, strakes and the plate was put down to a thickness within the material limit. In this research the main focus was on the plate materials. The mechanisms connecting the plates with the train were not discussed and also only the lateral pressure loads were discussed. The results of this work are finding a material that can result or maintain stability and light weight at the same time.[6]

Meng-ling WU†, Yang-yong ZHU, Chun TIAN, Wei-wei FEI: The title of the research is "Influence of aerodynamic braking on the pressure wave of a crossing high-speed train". The researchers used two trains passing each other. When aerodynamic braking works the wings can change the flow field around the train. Some studies have shown that aerodynamic impulsion caused by crossing high-speed trains can result in serious impact on the comfort and

safety noise, and windows being broken. In order to evaluate this issue they used two simulations by using a train with aerodynamic brakes and a train without aerodynamic braking.

The calculation model of the train was a simplification model of the China Railway High-speed (CRH) train. The researchers used the ICEM CFD software to partition the structured mesh and adopts O-grid structure to partition the vehicle and the brake wing. The sliding mesh technology is adopted to exchange the mesh information between two trains, and the sliding mesh model allows the adjacent meshes to slide. the result founded was When two trains with aerodynamic braking pass by each other, the highest crossing air pressure was 2 kPa; When a train passes by another one equipped with aerodynamic braking, the air pressure pulse around the train head will cause a positive low pressure area. Analogously, the air pressure pulse around the brake wing will cause a pressure-oscillation area on the surface of the train body; when two trains equipped with aerodynamic braking pass by each other, the pressure pulses of observation points not only appear at head and tail of the train, but also in the middle.

The middle pulses result from the brake wings. And the amplitude of the pressure pulses caused by brake wings is far less than those at the head and the tail; if the crossing train is not equipped with aerodynamic braking, pressure pulses will not appear except at the head and tail of the train. Thus, a train without aerodynamic braking will not impact the crossing train.

The researcher notes that in the future the limits of the maximum pulses related to different types of train should be considered .This will increase the safety. When installing an aerodynamic brake one should take account if the noise and the vibrations during crossing should be within the allowable limit.[14]

ZhuoJun Luo[1], Jianyong Zuo[1]*, Liguo Zhan2: The title of the research is" Simulation of Hydraulic System with AMESim for Aerodynamic Brake of High speed Train" .This research discuses about a hydraulic system that is designed in order to control the position of aerodynamic brakes The main energy source is from the trains air pipe and using oil in order to actuate the movement of the braking plates.

This research used the AMESim software but due to lack of some components in the library they were designed manually by using pneumatic component design. The design included two

parts the first part included the power source part and the second part included the functional part. The given design was tested by the software especially the displacement and velocity of the hydraulic cylinder piston. The given conclusion was the performance of the pressurized cylinder has met the design requests though the extreme value of its acceleration is a little high. Under the opening working condition, the hydraulic cylinder can finish its stroke in 3s, and the flow rate during opening is stable. Under unbalance load working condition, the flow rate and speed of the two hydraulic cylinders are a little different. From this research it can be recommended that there is a need for the modification of the system during unbalanced load position. [15]

From the aforementioned literature review, it can be concluded that in the application of aerodynamic brakes the following points should be well addressed. The first consideration is related to the installation of aerodynamic brake plates and the effective distance between them, it is noted that the distance should be minimum of 20m. The second consideration is when designing aerodynamic brake the structure should be as thin as within the material property limit .The thickness of the ribs and the hubs should also be as thin as possible. The third consideration is when the crossing of two trains with braking plates there will be a pressure wave that affects the safety. This results in the breaking of the window glass and also other parts resulting injuries. The fourth consideration is when designing the actuating mechanism the effectiveness should be checked by using working software's. If the above considerations are fulfilled it will result in an effective and efficient brake system.

In this research from Slavica Ristic the future work that is to determine the relationship between the drag force and the brake geometrical shape was taken into consideration .This is done by changing the braking plate arrangement. The second idea considered is the noise and two cars crossing each with braking plate.

CHAPTER THREE

3. SIMULATION AND METHODS OF THE STUDY

External aerodynamics is one of the main applications in the automotive industry. Engineers in the field of aerodynamics have been using CFD for a long time. Traditionally CFD is used to verify wind- tunnel experiments to optimize vehicle shapes in terms of lift and drag and study salient flow features in the last few years. The simulation of aero-acoustics has become another major application, which helps the aerodynamicist to obtain fast and reliable results for a specific configuration .To use CFD during design cycle one needs a reliable and straight forward approach which makes it possible to compare result for different vehicles and for several alternative vehicle modifications.

CFD is always subject to some constraints not only in the field of external aerodynamics. Among other constraints allocatable RAM total amount of CPU time and expected response time for results have to be taken into consideration. They determine the modeling approach used in terms of cell count and complexity of numerical models. This influences the accuracy of the results.

3.1. CFD, Theory and Governing Equations

3.1.1. CFD

Computational Fluid Dynamics (CFD) is the analysis of systems involving fluid flow, heat transfer and associated phenomena's such as chemical reactions by means of computer based simulation [7]

One of the biggest challenges in the engineering industry is being able to come up with efficient and optimal designs for new products. One of the strongest tools offered is FLUENT. FLUENT is a very useful program recently acquired by ANSYS. It has the capability to model fluid flow past objects with the ability to design, test, and analyze results all under one program [8]

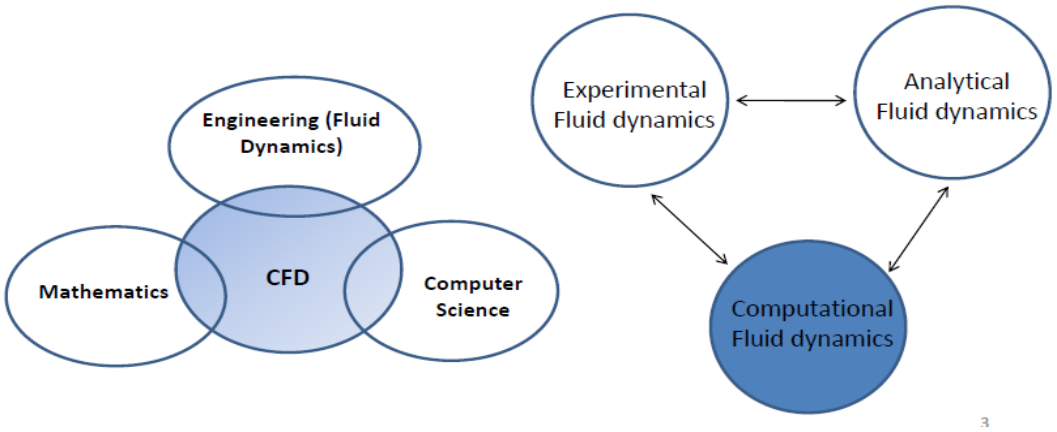

Figure 1: CFD

3.1.2. Theory and Governing Equation

ANSYS FLUENT is Computational Fluid Dynamics (CFD) software that allows users to simulate flow problems of ranging complexity. It contains broad physical modeling capabilities needed to model flow, turbulence, heat transfer, and reactions over objects designed by the user. Thousands of companies around the world benefit from the use of CFD software as a main part of their design phases in their product development. It uses the finite-volume method to solve the governing Navier-Stokes equations for a fluid which are derived from the conservation mass equation (1), the conservation of momentum (2) and the conservation of energy (3) equations. [9]

The difficulty arises from the fact that the conservation of mass, momentum and energy are coupled and non-linear set of differential equations making them practically impossible to solve analytically for practical engineering problems. Hence CFD software such as FLUENT is utilized to provide very reasonable approximation upon solving the specified governing equations [10]

Additionally, FLUENT also allows the users to model a range of flows such as incompressible or compressible, in-viscid or viscous, laminar or turbulent flow. The advanced solver technology that FLUENT has, provides fast and accurate results through flexible moving and deforming meshes to be able to create optimal designs. Ultimately, FLUENT allows engineers to design, create and analyze a configuration all under one program.

In order to model the object that a user wants to work with, its geometry and mesh must be first created in ANSYS Workbench. Another option is to import the geometry and mesh from Computer Aided Design (CAD) software packages such as Unigraphics, ProE or others. In Workbench, the user creates the object he or she wishes to analyze and Workbench guides the user through very complex metaphysics for fluid flow with drag and drop simplicity. Once the geometry has been created, the user can take advantage of several meshing options that Workbench provides. The user can implement the meshing in the specimen to analyze the structure as they try to analyze fluid flow past/through their object.

The conservation mass equation:

$$\frac{\partial \rho}{\partial t} + \nabla \cdot (\rho \vec{V}) = 0 \quad \ldots\ldots 1$$

The conservation of momentum equation:

$$\rho \frac{\partial \vec{V}}{\partial t} + \rho(\vec{V} \cdot \nabla)\vec{V} = -\nabla \rho + \rho \vec{g} + \nabla \cdot \tau_{ij} \quad \ldots\ldots 2$$

The conservation of energy equation:

$$\frac{\partial}{\partial t}\int e * \rho \, d\forall + \int (\breve{u} + \frac{p}{\rho} + \frac{V^2}{2} + gz)\rho \boldsymbol{V} \cdot \breve{\boldsymbol{n}} \mathrm{d}A = \dot{Q}_{net\ in} + \dot{W}_{net\ in} \quad \ldots\ldots 3$$

A few different ways of modeling and analyzing fluid flow are through turbulence modeling, k-ε, and y^+. Turbulence modeling is used to model turbulent flow. Turbulent flows are characterized by large, nearly random fluctuations in velocity and pressure in both space and time. These fluctuations arise from instabilities that eventually are dissipated (into heat) by the action of viscosity. Turbulent flows occur in the opposite limit of high Reynolds numbers. The two approaches to solving the flow equations for turbulent flow field can be roughly divided into two classes, direct numerical simulations and k-ε .[8] Direct numerical simulation numerically integrates the Navier-Stokes equations, resolving all of the spatial and temporal

fluctuations without resorting to modeling. k-ε, models Reynolds stress in two turbulent parameters, the turbulent kinetic energy (k) and the turbulent energy dissipation rate ∈ defined below by Equations 4 and 5 respectively.

$$\kappa \equiv \frac{1}{2}\left(\overline{u'^2} + \overline{v'^2} + \overline{w'^2}\right) \dots\dots\dots\dots\dots\dots\dots\dots\dots\dots\dots\dots\dots\dots\dots\dots\dots\dots\dots\dots\dots\dots\dots\dots\dots\dots\dots\dots\dots\dots 4$$

$$\epsilon \equiv \upsilon\left[\left(\frac{\partial u'}{\partial x}\right)^2 + \left(\frac{\partial u'}{\partial y}\right)^2 + \left(\frac{\partial u'}{\partial z}\right)^2 + \left(\frac{\partial v'}{\partial x}\right)^2 + \left(\frac{\partial v'}{\partial y}\right)^2 + \left(\frac{\partial v'}{\partial z}\right)^2 + \left(\frac{\partial w'}{\partial x}\right)^2 + \left(\frac{\partial w'}{\partial y}\right)^2 + \left(\frac{\partial w'}{\partial z}\right)^2 \right] \dots\dots\dots\dots\dots\dots\dots\dots\dots\dots\dots\dots\dots\dots\dots\dots\dots\dots\dots\dots\dots\dots\dots\dots\dots\dots\dots\dots\dots\dots 5$$

The next type of modeling is known as y^+. y^+ is a mesh-dependent dimensionless distance that quantifies to what degree the wall layer is resolved. y^+ plus is a non-dimensional parameter defined by Equation:

$$y^+ = \frac{\rho u y_p}{\mu} \dots\dots\dots\dots\dots\dots\dots\dots\dots\dots\dots\dots\dots\dots\dots\dots\dots\dots\dots\dots\dots\dots\dots\dots\dots\dots\dots\dots\dots\dots 6$$

Where u= $\sqrt{\frac{\tau_w}{\rho_w}}$ which is the friction velocity and y_p is the distance to the wall.

Workbench offers several meshing options, one being structured meshing. In structured meshing the user decides how many user defined shapes they want to place over the object they are analyzing. Structured meshing consists of tetrahedrons and exhibits a clearly pronounced pattern.

As the geometries increase in complexity it is necessary to adjust the meshing accordingly. However, when dealing with other cases such as flow across an airfoil, it is important to use a different mesh structure. One such structure is a structured "O- grid" around the airfoil. Because of the existence of the layers around the airfoil, it can be ensured the flow gradients are properly captured.

Fluent obtains a solution such that the mass, momentum, energy and other quantities are conserved for each cell.

The code of the CFD software solves directly the values of the flow variables at the cell centers and the values at other locations are appropriately interpolated[8] .In other cases, where there is no complicated geometry, but rather there is more flow gradients occurring around a certain area, the user can apply a bias.

Once the test object has been drawn and meshed in Workbench or imported from other software package (CatiaV5 for this paper case), FLUENT then allows the user to analyze it in different flow parameters. Another modeling capability FLUENT is capable of using is enhanced wall treatment. When the user chooses to use enhanced wall treatment, they can use this especially for turbulent cases using the k-epsilon model because it analyzes the object closer near the wall region.

The initial and boundary conditions can be specified in FLUENT and upon initializing the problem; it can be checked for convergence. If the convergence is not achieved accurate results will not be obtained. Finally, FLUENT provides a wide variety of parameters that can be plotted and analyzed.

In FLUENT during the obtainment of convergence the governing equations are solved for a predetermined by the user number of times (iterations). Specifically the magnitude of the average of particulate variable is computed as illustrated in Equation:

$$R = \sqrt{\frac{\sum_{i=1}^{N}(u_i - u_{gi})^2}{N}} \quad \ldots\ldots\ldots 7$$

Where R is the residual, N is the number of iterations to be performed, u indicates a particulate variable to be computed, and the subscript g indicates a guessed value

The incompressible Navier-Stokes equations in Cartesian coordinates are shown in Equations below.

X-direction: $\rho\left(\frac{\partial u}{\partial t}+u\frac{\partial u}{\partial x}+v\frac{\partial u}{\partial y}+w\frac{\partial u}{\partial z}\right)=-\frac{\partial p}{\partial x}+\rho g_x+\mu\left(\frac{\partial^2 u}{\partial x^2}+\frac{\partial^2 u}{\partial y^2}+\frac{\partial^2 u}{\partial z^2}\right)$ ……8

Y-direction: $\rho\left(\frac{\partial v}{\partial t}+u\frac{\partial v}{\partial x}+v\frac{\partial v}{\partial y}+w\frac{\partial v}{\partial z}\right)=-\frac{\partial p}{\partial y}+\rho g_y+\mu\left(\frac{\partial^2 v}{\partial x^2}+\frac{\partial^2 v}{\partial y^2}+\frac{\partial^2 v}{\partial z^2}\right)$ ……9

Z-direction: $\rho\left(\frac{\partial w}{\partial t}+u\frac{\partial w}{\partial x}+v\frac{\partial w}{\partial y}+w\frac{\partial w}{\partial z}\right)=-\frac{\partial p}{\partial z}+\rho g_z+\mu\left(\frac{\partial^2 w}{\partial x^2}+\frac{\partial^2 w}{\partial y^2}+\frac{\partial^2 w}{\partial z^2}\right)$ …10

Drag and lift

The Drag Force, D, acts in the direction of the free stream while the Lift Force, L, is normal to the free stream. Objects such as airfoils are designed to generate lift. However for objects such as cars, trains, it is desired to reduce the lift since the lift on a car or train reduces the contact force between the wheels and the ground or rails. Typically the lift and drag are given in terms of the Coefficient of Lift and the Coefficient of Drag which are dimensionless forms of the Lift and Drag forces.[11]

$$C_L=\frac{L}{0.5*\rho*U^2*A} \quad \ldots\ldots\ldots\ldots\ldots\ldots\ldots\ldots\ldots\ldots\ldots\ldots\ldots\ldots\ldots\ldots\ldots\ldots\ldots\ldots\ldots\ldots\ldots\ldots\ldots\ldots\ldots\ldots 11$$

$$C_D=\frac{D}{0.5*\rho*U^2*A} \quad \ldots\ldots\ldots\ldots\ldots\ldots\ldots\ldots\ldots\ldots\ldots\ldots\ldots\ldots\ldots\ldots\ldots\ldots\ldots\ldots\ldots\ldots\ldots\ldots\ldots\ldots\ldots\ldots 12$$

3.2. Aerodynamic Drag

3.2.1. Formation Mechanism of Train Aerodynamic Drag

In the open air condition, the aerodynamic drag of the train is the sum of the tangential forces (skin friction drag) and the normal forces (pressure drag), both of which are parallel to the opposition direction of vehicle's velocity vector[12]. The pressure drag comes from the integral of the skin pressure of the train. The direction of drag is along the positive direction of x axis, as shown in Figure 2 below. The friction drag can be obtained by the integral of the tangential forces. The drag formula for the train in the open can be expressed as:

$$F_x = F_{px} + F_{\tau x} \quad \ldots\ldots\ldots\ldots\ldots\ldots\ldots\ldots\ldots\ldots\ldots\ldots\ldots\ldots\ldots\ldots\ldots\ldots\ldots\ldots\ldots\ldots\ldots\ldots\ldots\ldots\ldots\ldots 13$$

Where $F_x$the aerodynamic is drag, F_{px} is the pressure drag and $F_{\tau x}$ is the friction drag.

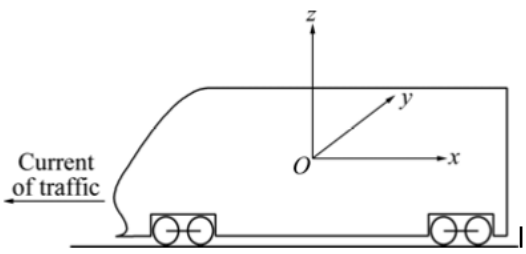

Figure 2: Coordinate Definition of Train

Therefore, the aerodynamic drag on the traveling train is divided into pressure drag and friction drag. The formation mechanism of the aerodynamic drag will be discussed in the following part.

3.2.2. Composition of Aerodynamic Drag

The train drag is divided into the aerodynamic drag, the sliding force between the wheel and rails, and the friction force caused by the pantograph system. The total drag of train was composed of the sum of each carriage drag.

3.2.3. Relationship between Aerodynamic Drag and Total Drag of Train

In the open air condition without any cross-wind effect, the total drag on the traveling train can be expressed by Davis experience formula (12):

$$F_R = a + bvt + c{v_t}^2 \quad \ldots \ldots \ldots \ldots \ldots \ldots \ldots \ldots \ldots \ldots \ldots \ldots \ldots \ldots \ldots \ldots \ldots \ldots \ldots \ldots \ldots \ldots \ldots \ldots \ldots \ldots \ldots \ldots \ldots 14$$

Where F_R is the total drag, a, b and c are the constants determined by the experiment, and v_t is the train velocity relative to the ground.

In general, in Eqn. 14 (above), the total drag can be divided into two contributions: $a + bv_t$is the mechanical drag which includes the sliding drag between rails and train wheels, and the rotating drag of the wheels; and $c{v_t}^2$is the aerodynamic drag. So the aerodynamic drag can be expressed as:

$$F_x = cv_t^2 \quad \ldots\ldots 15$$

The coefficient of aerodynamic drag (c_x) can be described as:

$$c_x = \frac{F_x}{qs_x} \quad \ldots\ldots 16$$

Where q is the dynamic pressure, and s_x is the cross-sectional area of the train.

Therefore, the aerodynamic drag can be written as

$$F_x = qs_x c_x = ½\rho s_x c_x v_t^2 \quad \ldots\ldots 17$$

Compared with Eqns.(15) and (16), the coefficient (c)can be expressed as:

$$c = \frac{1}{2}\rho s_x c_x \quad \ldots\ldots 18$$

The aerodynamic drag is proportional to the square of speed of the strain, while the mechanical drag is proportional to the speed of the train. Compared with the mechanical drag, the portion of the aerodynamic drag becomes larger as the train speed increases.

3.2.4. Relationship between Aerodynamic Drag and Each Carriage Drag of Train

The aerodynamic drag of the train is composed of the drag of each carriage. The drag force can be written as:

$$F_x = F_{xt} + \sum_{i=1}^{n} F_{xz}(\text{i}) + F_{xw} \quad \ldots\ldots 19$$

Where$F_x$is the total aerodynamic drag; F_{xt} is the drag of the leading car or locomotive; F_{xw} is the drag of the tail car; F_{xz}(i) is the friction along the train, which includes the bogies, wheels, interference, and bottom structure of the train; and n is the number of middle carriages. The coefficient (c_x) can be written as:

$$c_x = c_{xt} + \sum_{i=1}^{n} c_{xz}(\mathrm{i}) + c_{xw} \quad \ldots\ldots\ldots\ldots\ldots\ldots\ldots\ldots\ldots\ldots\ldots\ldots\ldots\ldots\ldots\ldots\ldots\ldots\ldots\ldots\ldots\ldots\ldots\ldots\ldots\ldots\ldots\ldots 20$$

Where c_{xt} is the drag coefficient of the leading car or locomotive; c_{xw} is the drag of the tail car; and c_{xz}(i) is the friction coefficient along the train, respectively.

3.2.5. Formation Mechanism of Pressure Drag

When the train runs at high speed, there will be a stagnation region with high pressure on the windward face of the train nose, and the flow speed will decrease. At the same time, the flow moves at high velocity along the tail car and the pressure decreases. The pressure drag stems from the pressures due to the abrupt change in the cross-sectional area of the train. The pressure drag can be obtained by integrating along the whole car

$$F_{px} = \oint_{SF} p_{bx} d\, s_F \quad \ldots\ldots\ldots\ldots\ldots\ldots\ldots\ldots\ldots\ldots\ldots\ldots\ldots\ldots\ldots\ldots\ldots\ldots\ldots\ldots\ldots\ldots\ldots\ldots\ldots\ldots\ldots\ldots 21$$

Where,$p_{bx}$is the skin pressure of the train along x axis, and s_F is the area of the train wall surface`.

For the train, the pressure drag comes from the pressure due to the shape of fore-body and after-body of the train, the connecting parts between trains, the train wall surfaces, the pantograph system, the bogie, and underneath structure of the train. The mechanism of forming pressure drag is given as follows: there is a stagnation region in the leading car nose and air guide sleeve. The flow velocity of air is almost equal to zero, when the pressure reaches the largest in these regions. The flow around the pantograph system and bogie can also cause the increase of the skin pressure and the decrease of speed. And there are large pressure changes in the connecting parts between trains. When the air flow along the train reaches the end car, the flow speed will increase and the pressure will decrease. Air flow separation occurs at the nose of the end car. This results in a great change in the pressure distribution at the end car, leading to the pressure drag.

3.2.6. Formation Mechanism of Friction Drag

Due to the viscosity of the air, boundary layer occurs on the wall of train when the air flows along the train (12) the height of boundary layer is equal to zero at the nose of the train, and becomes larger at the leeward. The speed of flow increases from zero to running velocity of the train along the boundary layer normal direction. The tangential forces are caused by the difference of the velocity in the boundary layer normal direction, which is shear stress on the train surface. Friction drag of the train is the sum of shear stress, which is in the reverse direction of the train running direction. Friction drag can be obtained by integrating along the whole train:

$$F_{\tau x} = \oint_{SF} \tau_{ix} ds_F \quad \ldots\ldots\ldots\ldots\ldots\ldots\ldots\ldots .22$$

Where, τ_{ix} is the shear stress on the train along x-axis

The shear stress is proportional to the viscosity of the air (μ) and the velocity gradient. The velocity is related to the height of boundary layer. However, the boundary is closely related to the shape of the train, the smooth of the train wall, the running velocity and the ambient surround. Therefore, the friction drag is relevant to the shape of the train, the smooth of train surface, the running velocity and the ambient surround.

3.3. Aerodynamic Plate size determination

This braking device is purely an aerodynamic device .the aerodynamic plate can be rectangular plate or a curved plate. The most widely used and easily manufactured type is the rectangular plate. This type also has a large drag coefficient that is highly chosen for this type of train braking.

Aerodynamic braking devices have been used on electric trains of modern railway industries. These brakes are widely used on HST when speed increases the drag force will increase at a speed of 120km/hr. The percentage of drag force from total forces becomes 40% on high speed

trains without aerodynamic braking. The emergency brakes are replaced with other type of braking system but the aerodynamic braking play a major role due to the relationship between the speed of train and drag resistance.

The primary considerations to locate the device as close to the tip as much as possible for maximum aerodynamic effectiveness and also should be of minimum overall weight.

There are different types of plates used in aerodynamic brake. For this paper rectangular plate is chosen due to its high drag coefficient and also easy manufacturing. The following constraints should be considered when choosing the area.

- The height of the pantograph from the rail end
- The width of the train

The given dimensions are:

- The height of the pantograph from rail end is 5700mm.
- The height of the train 4433mm.
- The available width of train is 2305.

The dimension of the plate is found to be 900mm×1600mm×120mm

3.3.1. Energy

The energy dissipated during the usage of the braking plate can be found by using the drag force .the energy is found to be

$$E = \frac{1}{2}m(v^2 - u^2)$$

The running velocity is 34m/s and the end velocity is 8.4m/s. The pay load of the train is found from the specification to be 25000kg.By using the above parameters the energy becomes to be

$$E_{120} = 27136kJ$$

$$E_{300} = 171MJ$$

3.3.2. Pitching moment

While the lift force acts to decrease (or increase) the weight on the axles, the pitching moment acts to transfer weight between the rear axles. Pitching moment arises from the fact that the drag does not act as the ground plane (thus it accounts for the elevation of the drag force) and the lifting force may not act exactly at the center of the wheelbase. Pitching moment is described by the equation:

$$PM = \frac{1}{2} * \rho V^2 * \mathrm{Cpm} * \mathrm{A} * \mathrm{L}$$

The calculated pitching moment becomes $PM_{120} = 3915Nm$

$$PM_{300} = 23681Nm$$

3.4. Geometry cleanup and preparation

Most of the car geometries that are analyzed today are close to the production shape, which is highly detailed within all areas. During the CFD- treatment the necessary simplifications should be as few as possible. The creation is predominantly carried out by surface based CAD-systems due to their complexity .Unfortunately these do not guarantee closed surfaces.

On the other hand volume based modeling systems have the advantage of the outer surfaces being inherently closed. The eventual goal of expanding the typical vehicle model so that it includes such features as detailed underbody and all under-hood components is a limitations of such systems .

During the preparation for a flow-simulation, a consistent definition of fully connected geometry has to be ensured. This first step comprises a cleaning up of the CAD model and is totally independent of the subsequent method of simulation suitable tools for this process would include the original CAD systems used for definition (CATIA,IDEAS,UNIGRAPHICS,)as well as FE- post-processing programs (ANSA, CATIA- and IDEAS-mesher, PATRAN) For dealing with simple volume –based geometry definitions as well as for simple surface- based models fluent's preprocessor GAMPIT can be used .to be

successful with highly complex shapes the usage of an FE-preprocessor like ANSA might be necessary.

3.4.1. Vehicle geometry

The surface mesh must be as smooth as possible to allow prism layers to be extruded from the surface of the car (except the underbody if it is too complex).Sharp angles must be avoided .The creation of additional faces ,which later will be treated as" interior", is a trick to close or smooth out those regions. TGrid can then be used to fill the gap between these additional "membrane-like "interior faces and the real surface of the car with tests. Cavities like air intakes should be closed in a similar way and treated as separate volumes during volume meshing.

The vehicle geometry is done by using CATIA .The basic dimensions were taken from ERC. The detail dimensions were not given as a result the dimensions were estimated by the drawing and the standard train dimensions. The braking plate was assembled on the train in four different angles. This is done in order to compare the drag force at different arranagements and also which assembly has the best optimum moment and drag force effect. The geometries are shown below.

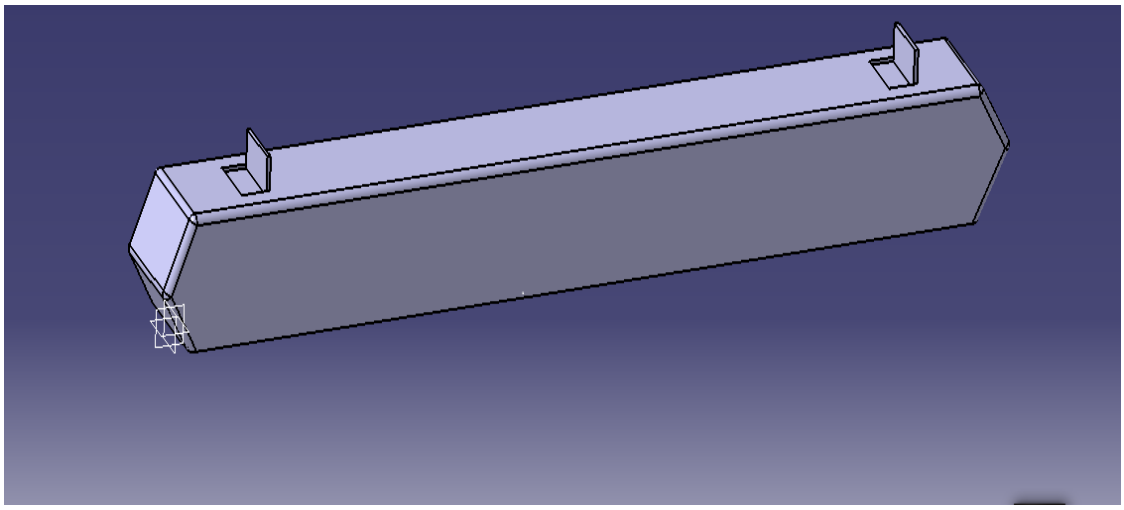

Figure 3: Braking plate at angle of 90^0

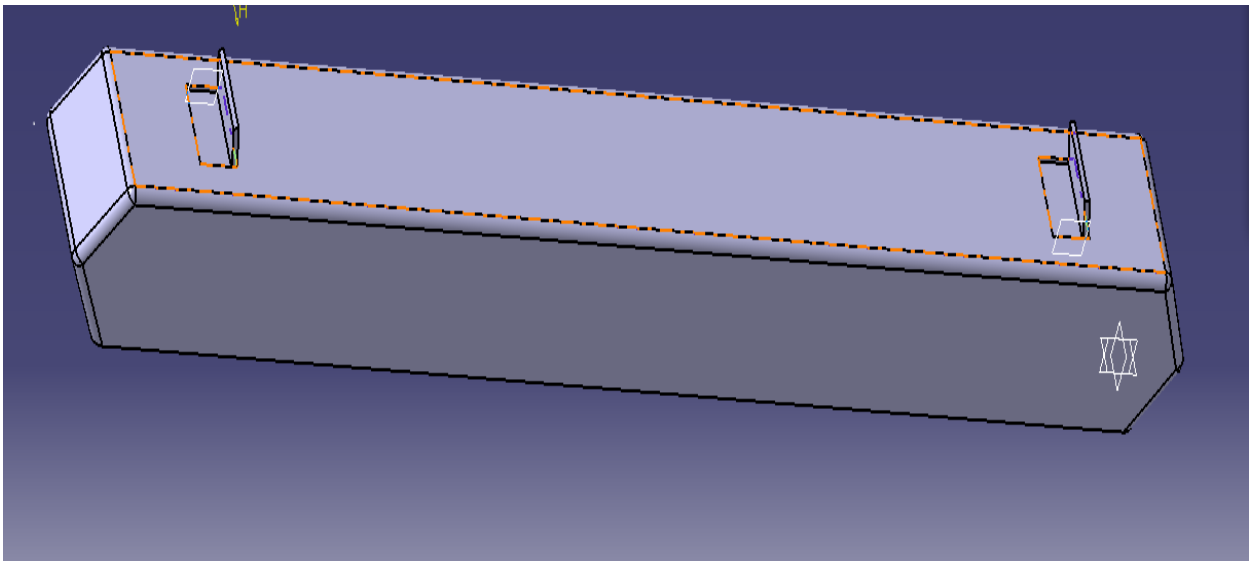

Figure 4: Braking plate at angle of 75^0

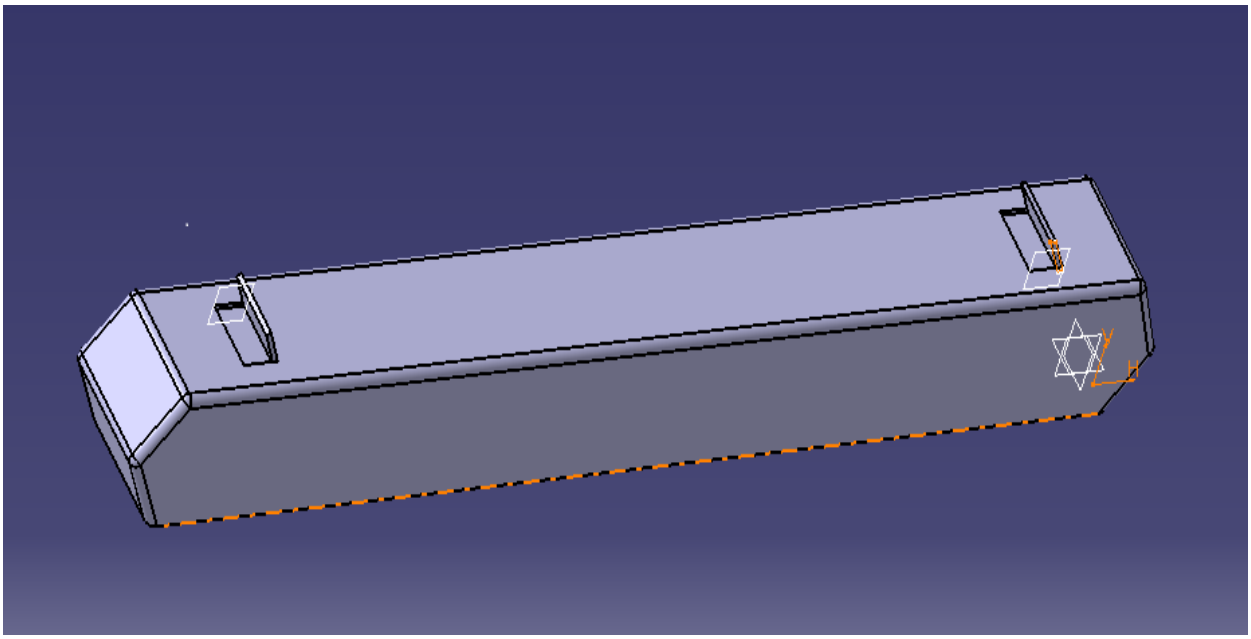

Figure 5: Braking plate at angle of 60^0

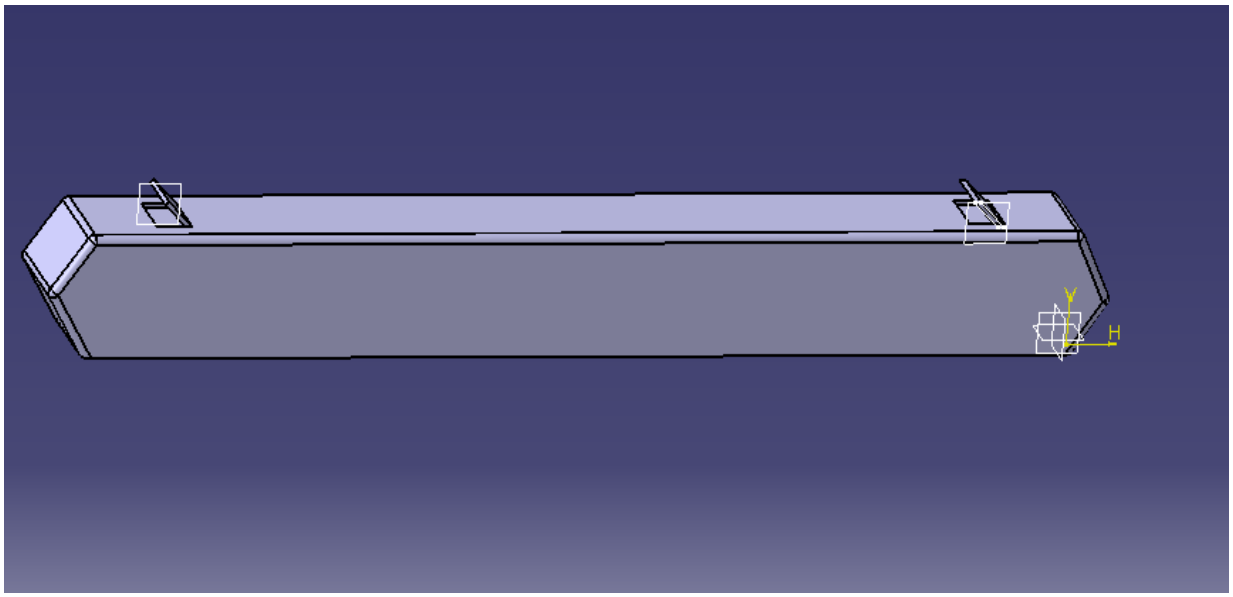

Figure 6: Braking plate at angle of 45^0

3.4.2. Computational domain (wind tunnel)

The computational domain is extended by two lengths of train both upstream and downstream of the train. The total length of the computational domain is around 3 times the length of the train. The computational domain is also extended in the transverse directions by 0.5 times the length of the model each on either side of the train. The height of the computational domain is also extended by about 0.5 times the length of the model. The boundary is shown below.

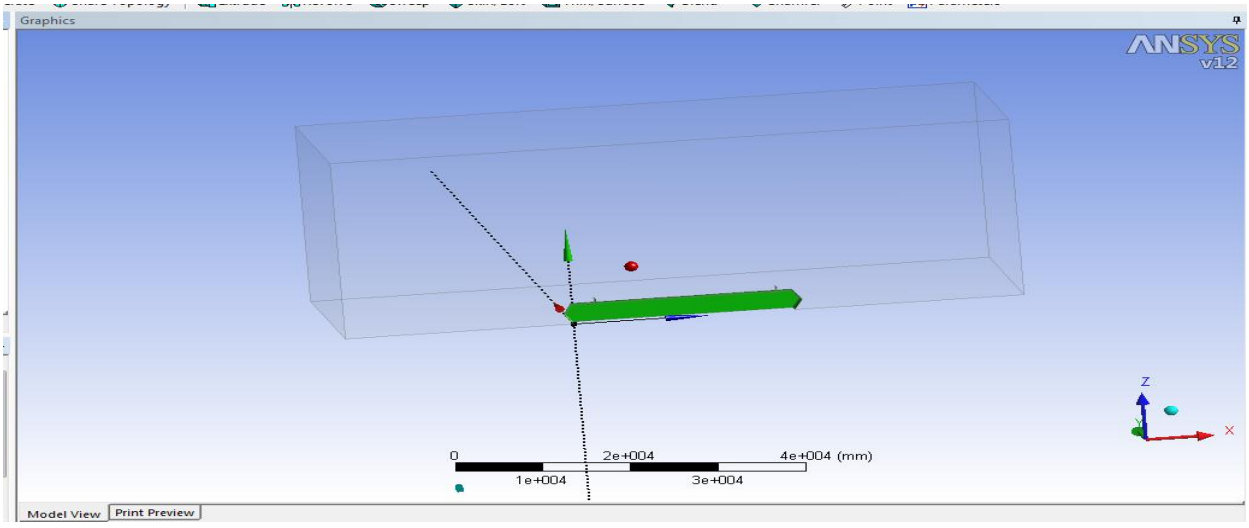

Figure 7: Boundary condition

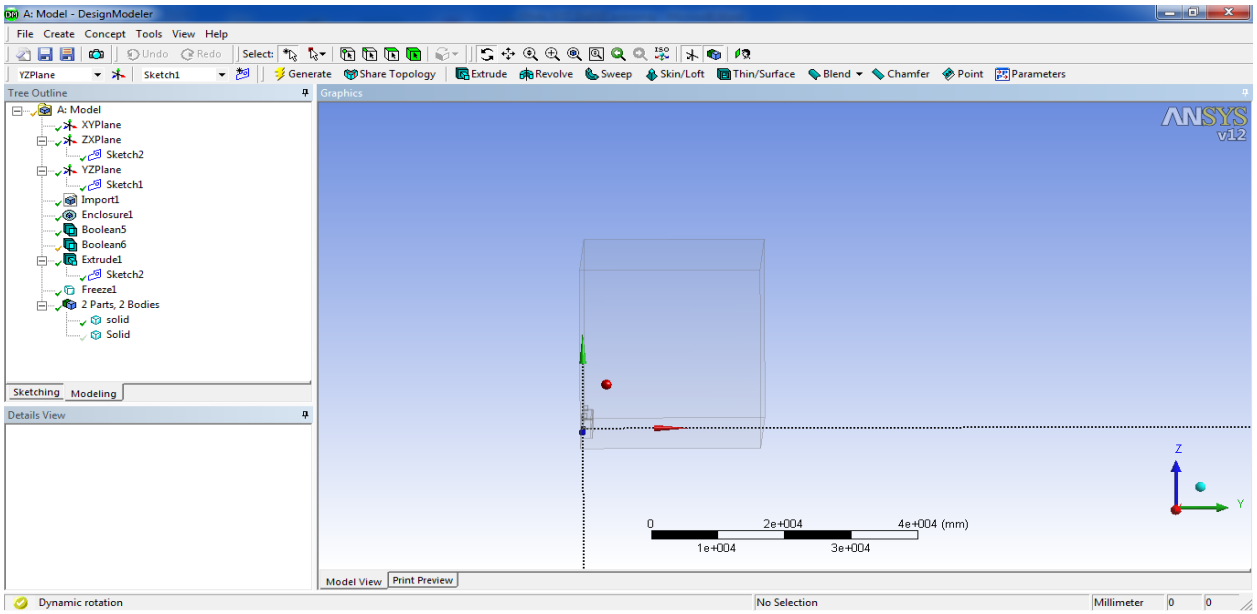

Figure 8: The boundary for the vehicle

3.5. Meshing

3.5.1. Meshing strategies

In general there are three different strategies to create the volume mesh for simulations in FLUENT

- Strategy A(adaptation)
- Strategy B(boxes)
- Strategy C(controls)

Strategy A

This simulation strategy uses the adaptation functionality in the fluent solver. a relatively coarse mesh is used as a starting point and a first solution is calculated. To complete the simulation several static pressure gradient adaptations are necessary. In each adaptation cycle about 1.3% of the total number of cells should be refined using the hanging nodes adaptation method in FLUENT. Then further iterations are needed until convergence of drag and lift coefficients is achieved. Overall 3 to 5 adaptation cycles may be necessary to reach a state

where the force coefficients or any other important parameter will no longer be subject to any significant changes.

In order to decrease the total number of cells, the cells to be adapted (marked) can be limited to a region not too far from the car .To do so, You must create one register using static pressure gradient and another grouping the cells inside a hexahedral region near the vehicle

Strategy B (boxes)

This strategy is based on internal boxes created around the vehicle and in the wake region to explicitly control mesh size. This approach is more time consuming than strategy A. but very accurate .The boxes are typically created in the post processing tool. A constant size of surface elements is applied to the box walls. The boxes are used in Tgrid as meshing domains, in which cell size can be controlled in a very comfortable way. Another advantage of this method is the possibility to combine different meshing techniques in one model. Hence hex meshes can be used for the outer region of the wind tunnel and can be kept for a different simulation while only the inner box is changed. The connection between those boxes can be either conformal using pyramids or non-conformal by using the interface definition of FLUENT.

Strategy c (controls)

In this strategy the internal boxes are replaced by virtual boxes used for cell refinement in t grid therefore the local refinement functionally Tgrid is used. This approach can either be used for general tetrahedral or hex core meshing. These methods will be described in the volume meshing section of this document. This approach is very accurate and avoids the creation of additional surfaces in prior steps. This strategy is recommended by fluent.

3.5.2. Volume meshing

Volume meshing comprises of two main steps. To ensure low skewness elements where viscous effects are large, prism elements are extruded from the car surface in a first step. Following this the rest of the domain is filled either with hexahedral and /or tetrahedral elements.

Mesh setup

By using the above basic mesh setup systems for this locomotive the following steps were used

1. Automatic meshing: this is done to see what ANSYS can do by itself and to analyze what to modify.
2. Size control or strategy c from above: in this step mesh control was done by making the proximity and curvature from advanced setting and activating medium smoothing. The maximum and the minimum cell size being 0.1m and 2.5 respectively. Growth rate was also set into 1.2. In the sizing part another rectangle was being drawn around the main body in order to set a body of inference.
3. Body and face sizing: the braking plates were with an element size of 0.02m .other bodies were sized into an element size of 0.1 m.
4. Inflation (prismatic layers)-this was done on the boundary by program controlled type and setting the smoothing iteration to be 10.
5. Named selections-this is mainly useful in the solution part to do the analysis part on. These named selections are the locomotive body as inert body .The symmetry faces at both sides and top of the boundary or the air volume with no slip condition. And at last the bottom is assigned as road.

   The meshed body is shown below

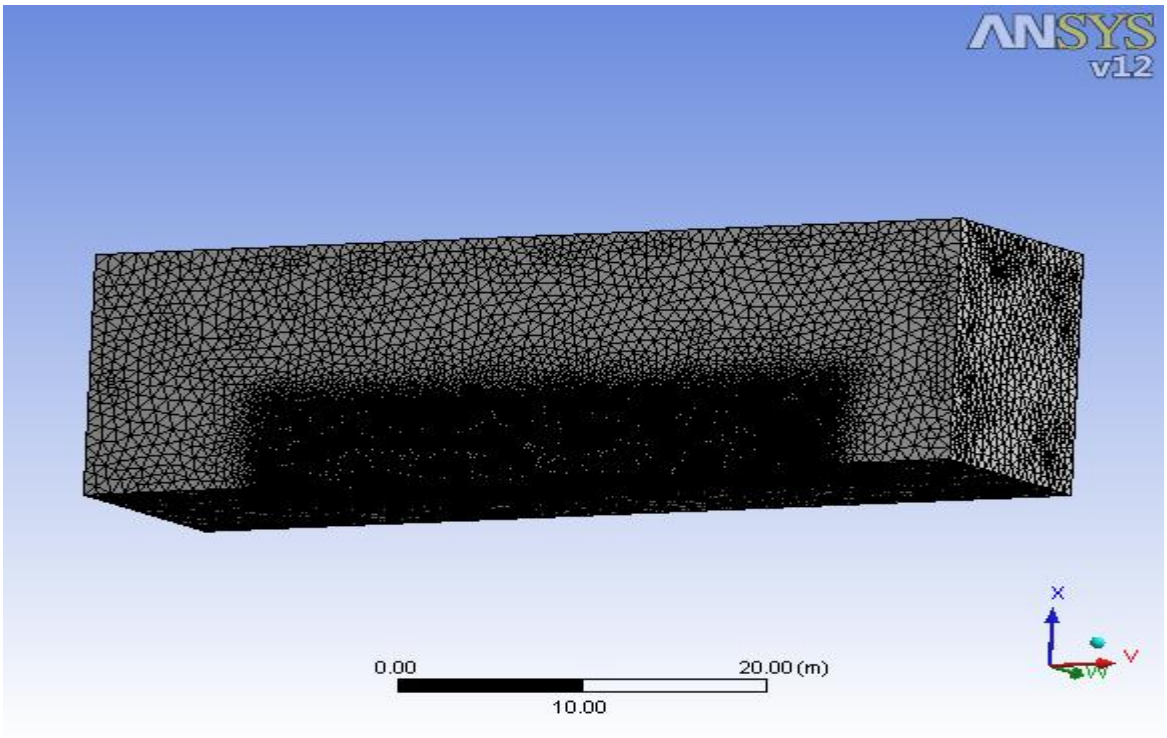

Figure 9: Meshing A

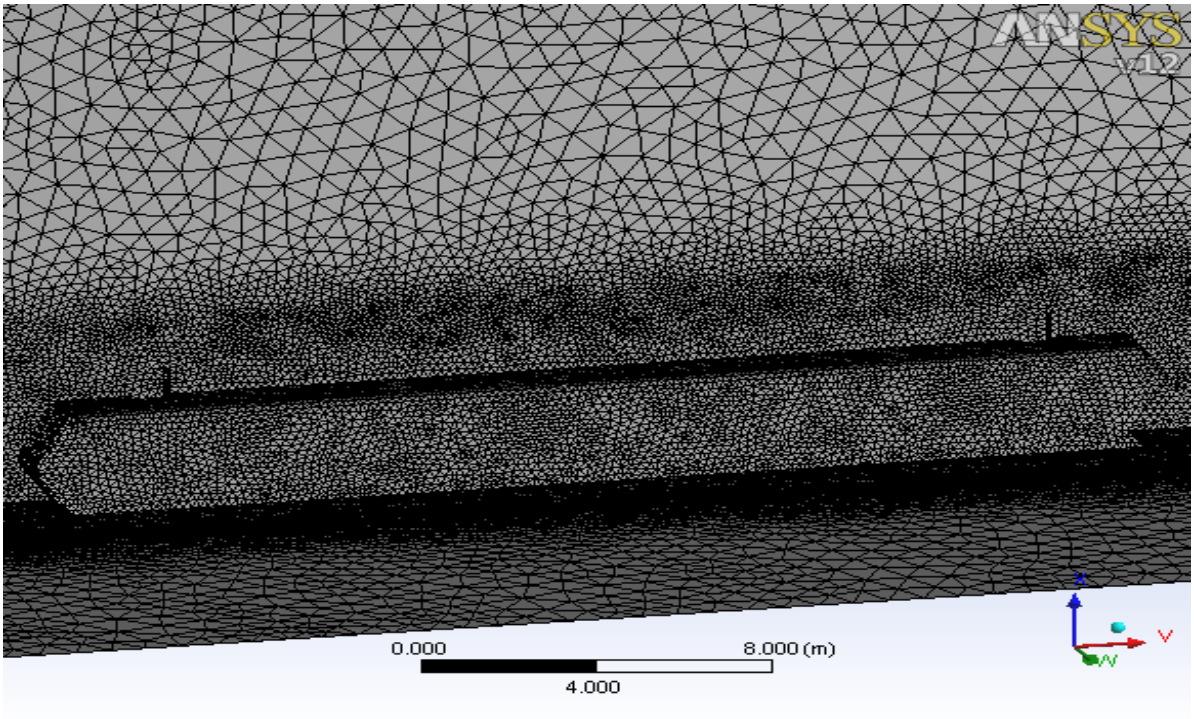

Figure 10: Meshing B

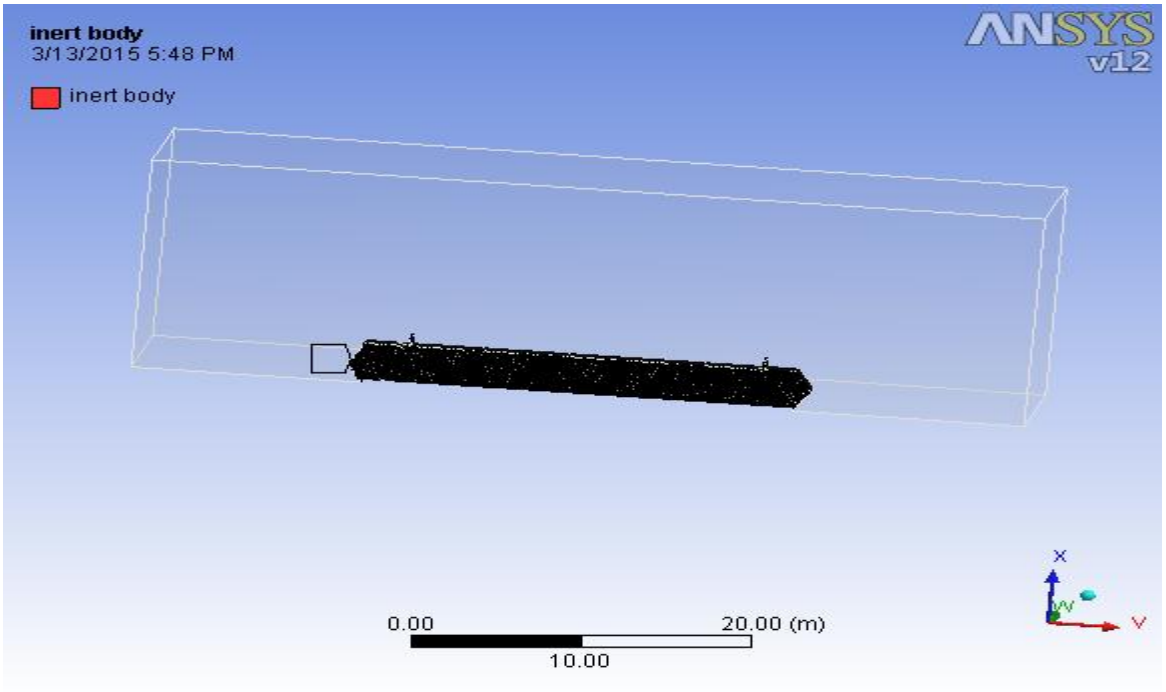

Figure 11: Inert body

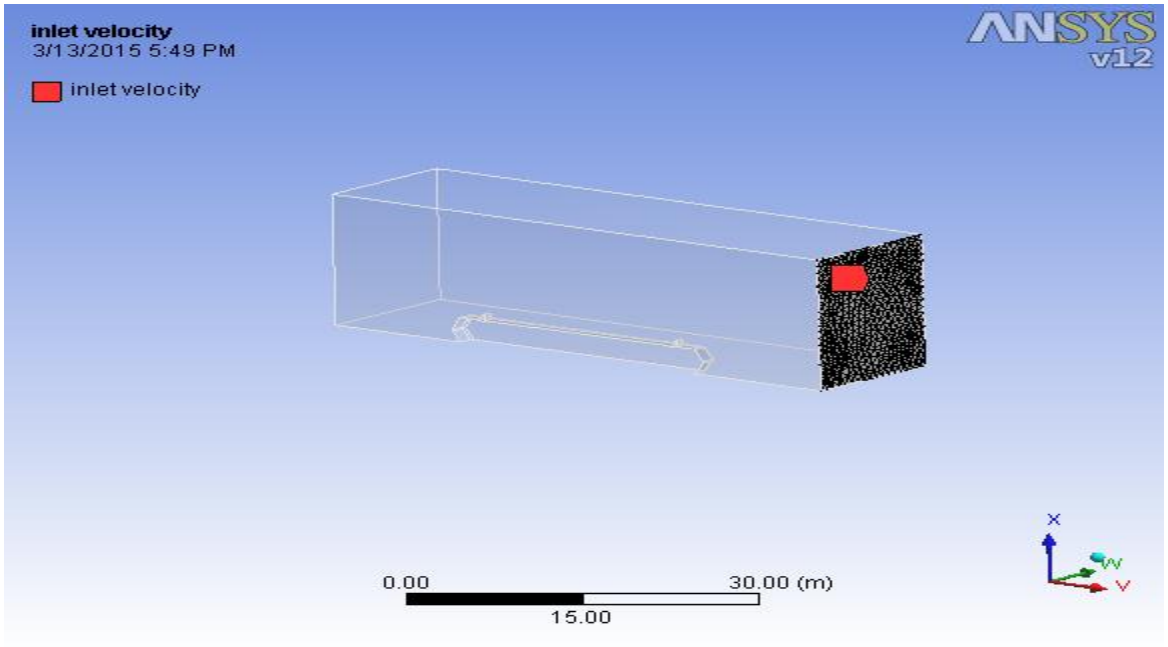

Figure 12: Inlet velocity

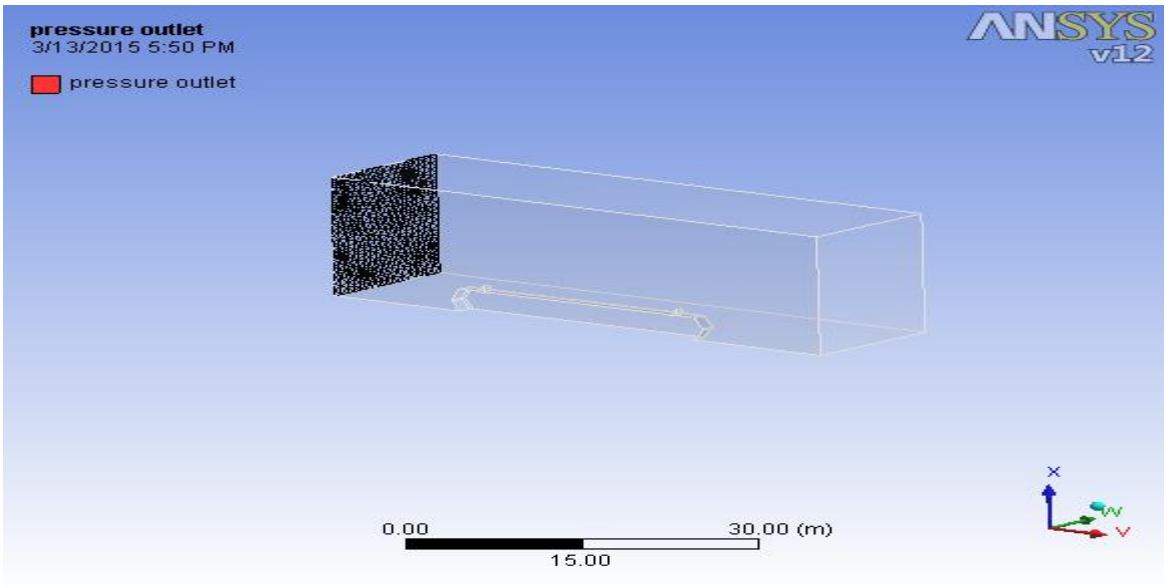

Figure 13: Pressure outlet

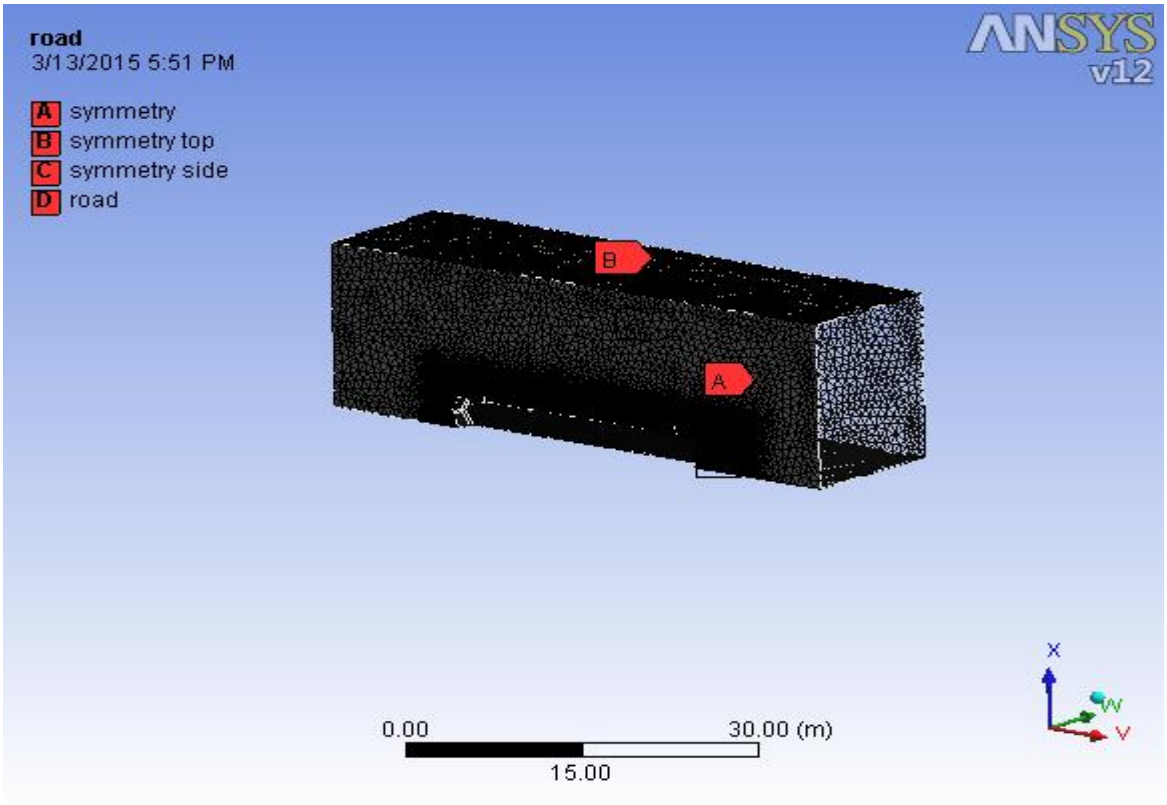

Figure 14: symmetry

3.6. Solving

3.6.1. Boundary conditions

The specifications of boundary conditions should be geared as close as possible to the measurement conditions in the wind tunnel. In the majority of cases, flow velocity and turbulent intensity of the wind tunnel are known. Therefore a velocity-inlet boundary condition is used to model the incoming flow. Velocity magnitude and the flow direction are specified. Completed with turbulent values at the inlet. The user can choose between several options to specify those effects like rotating wheels and moving belt can be modeled using the moving /rotating wall boundary condition. This adds tangential velocity to the selected walls .in cases where the boundary layer suction is present, the relevant areas have to be defined as separate wall zones and shear stresses have to be set equal to zero. Specify a symmetry boundary condition for the rest of the domain.

Turbulence modeling

The fidelity of CFD predictions for turbulent flow is highly dependent upon the quality of the turbulence modeling. This is even more important for the flow around ground vehicles, whose salient flow features includes three-dimensional boundary lines with strong streamline curvature Separation and strong vertices. These features require turbulence models that can properly account for non-equilibrium effects and anisotropy.

Based on experience, Fluent recommends two types of turbulence models for external aerodynamic studies.

Realizable k-epsilon model

The realizable k-epsilon model proposed by shih et al.[5] is intended to address the well-known deficiencies of traditional k-epsilon models by adopting the following:

- A new eddy-viscosity formula involving a variable for c_{mu} originally proposed by Reynolds

- A new model equation for dissipation based on the dynamic equation of the mean square vortices fluctuation.

Industrial applications of this model show that it is possible to achieve good results in terms of integral values (e.g. drag coefficient),which are within 2-5% due to its implementation it is very stable and fast converging. Therefore it is perfectly suited for automated calculation processes, allowing a huge number of calculations in a relatively small time frame

Reynolds stress model (RSM)

In the last few years, the employment of second- moment closure models in which transport equations for the individual Reynolds stresses are solved ,has become more and more widespread. RSM rigorously accounts for anisotropy of turbulence and the transport of all Reynolds stresses. But these advantages come at the price of higher cost in computational time (+40%) and RAM resources (+20%). The RSM Model in FLUENT 6 is based on the models of Gibson and Launder [6] and, more recently, speziale et al. [7] and it is implemented in the framework of an unstructured mesh. RSM is recommended for high-fidelity simulations, in which salient flow features and structures are studied and compared.

If RSM is applied, it is recommended to use the following settings

- Initialize the flow field (do not use flow field calculated using a 2-equation model)
- Set under relaxation factors to :
  - ✓ 0.65 for pressure.
  - ✓ 0.5 or momentum and
  - ✓ 0.5 for k and epsilon
- Change formulation for the epsilon-equation for external aerodynamics with RSM, by setting the following SCHEME commands:
  [**rpsetvar'drsm/coupling-alt-average?#]**
- Request 50 iterations with first order discretization, then switch to second order
- If convergence problems occur right at the beginning of the calculation, set under relaxation factors for k and epsilon to 0.2 for 50 iterations, then switch to 0.5 and after that switch to second order discretization.

For high Reynolds Number Flows, such as flows around ground vehicles, it is a well-recognized fact that resolving the near-wall region down to the wall is not practical. Therefore semi-empirical wall functions are used. To overcome the well-known drawbacks of traditional wall-functions FLUENT offers non-equilibrium wall-functions (NWF'S).Besides being sensitized to the effects of pressure gradients. NWF'S account for the effects of local variation in the thickness of viscous sublayer, When computing the turbulent kinetic energy budget un wall-adjacent cells.

It is strongly recommended that NWF'S be selected for external-aero simulations. Compared to the traditional all functions. NWF'S provide more realistic predictions of the behavior of turbulent boundary layers, including flow separation , and they do so without a significant increase in either CPU-time or dynamic memory.

Steady state calculation

Use the following procedure to start the simulation:

- Make sure that all boundary conditions are accurately denied
- Define Non-conformal interfaces(if existent)
- Enable second order upwind for momentum, turbulence. Kinetic energy and turbulence dissipation rate.
- Initialize the flow field with zero velocity and turbulence values from the inlet
- Activate monitors for lift and drag of the vehicle (make sure that reference values are set properly)
- Define monitor points for pressure or velocity at a particular point in the wake region
- Request iterations
- Carry on calculation until all monitors show constancy.
- Check plausibility by plotting cp,compare cd and cl to widow tunnel results
- Check for y+values (30-300)

Solution setup

In the solution set up the following steps are taken in order to achieve the results.

1. The first step is checking the mesh in the general part: this step is useful especially when the meshing was done by other programs and imported into ANSYS Fluent.
2. This step is for choosing models the Realizable k-epsilon model is chosen for the advantages listed above.
3. Choosing of material which is in this case fluid (air).
4. Boundary conditions: in this steps the boundary conditions in ANSYS meshing are connecter or change in solution sense. The use of naming relatively will help in solution to be sensible automatically. The symmetry is same as symmetry in solution the changes made are in the inlet velocity and pressure outlet. inlet velocity the running velocity is entered which is 34m/s in this case .the specification method is changed into intensity and viscosity ratio and also set turbulence intensity and turbulent viscosity ratio to be 1% and 10 respectively. The second one is the pressure outlet in which the turbulence intensity and turbulent viscosity ratio to be 5% and 10 respectively.
5. Solution method: the spatial discretization is done on least square cell base gradient the momentum, turbulent kinetic energy and turbulence dissipation rate are set as a first order upwind. This is done due to the capacity of the computer if it is set into second order it will take more memory making it difficult for the computer to solve.
6. Monitors: this will help on which solution needs to be displayed during iteration the displayed results include residuals drag coefficient, lift coefficient and also moment coefficient
7. Initialization: before solving initialization is an obligation this step will make clear to the system from where to where the solving is done.
8. The final step is listing the amount of iteration to be 500 and computing the solution.

3.7. Influence of aerodynamic braking on the pressure wave of a crossing train

When aerodynamic braking works the braking wings can change the flow field around the train. Some studies have shown that aerodynamic impulsion caused by crossing high-speed trains can result in serious impact on the comfort and safety including oversize deformation, loud noise, and windows being broken. This section focuses on the characteristics of the pressure pulse of crossing high-speed trains

3.7.1. Modeling of the train

The model is done by using CATIA. The train dimensions are the same as before and also the meshing setup and solution setup are taken to be the same as the above. The simulation is taken at the plate arrangement of 90^0 because it is with highest braking plate area.

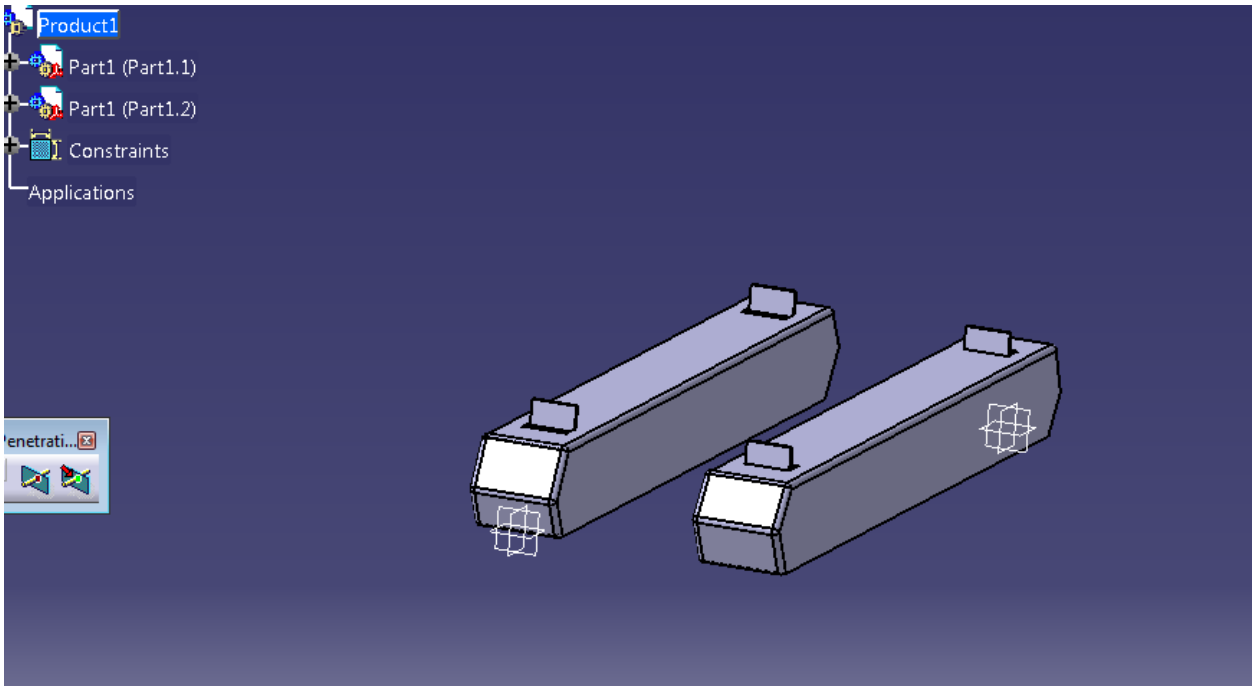

Figure 15: Modeling of crossing train

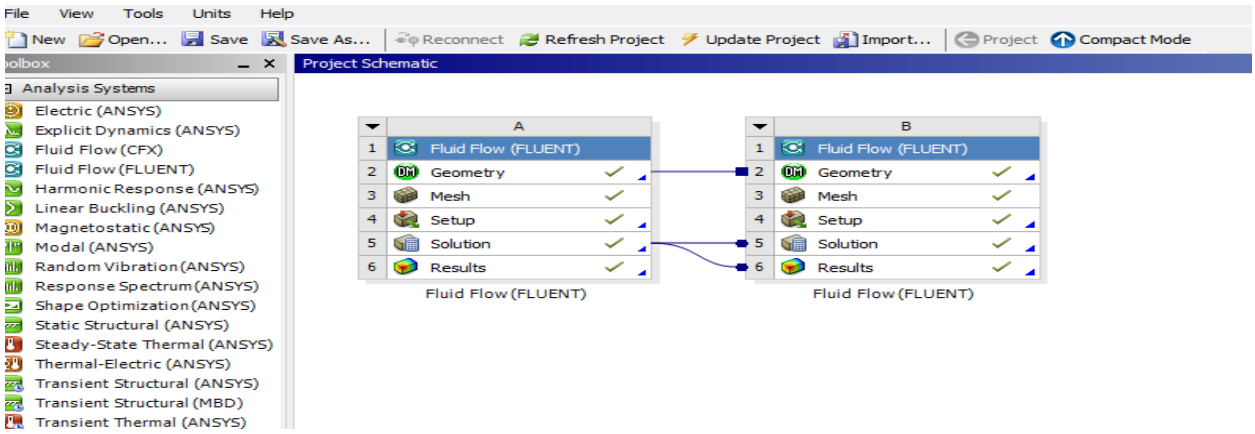

Figure 16: Analysis of crossing train

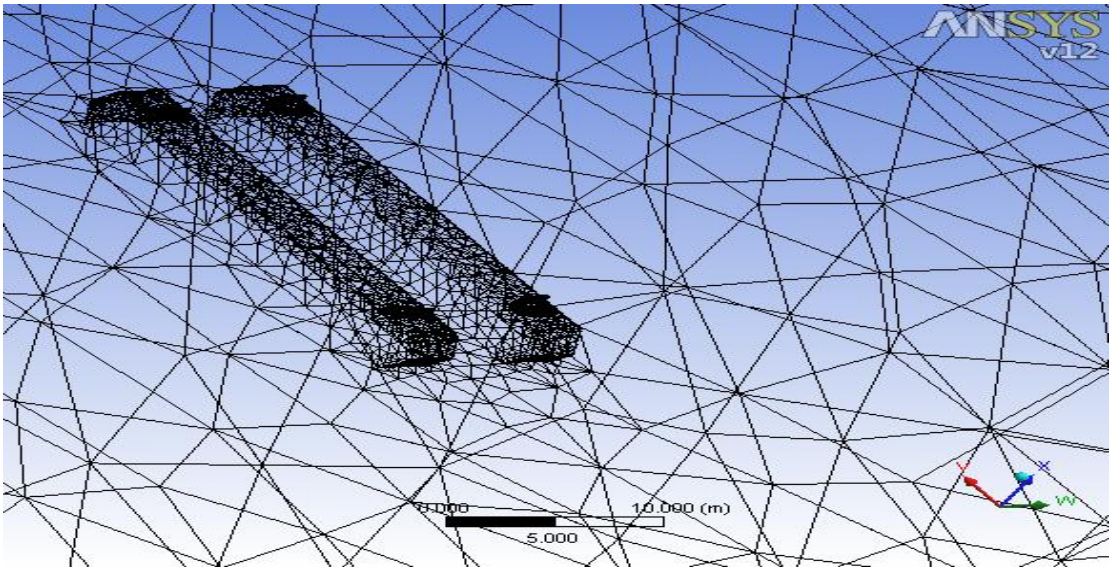

Figure 17: Meshing of crossing train

CHAPTER FOUR

4. RESULTS AND DISCUSSIONS

The results are done on two different velocities. The first one is the 120km/hr which is the running speed for the current train when starting work .the second speed is 300km/hr this speed is the future plan for high speed train on that same route. The results are analyzed below.

4.1. Cm (Pitch moment)

The lift force, L, is the result of integrating a distributed force over the surface of the train. This distributed force is equivalent to L, acting through a particular point called the center of pressure. For symmetric sections, changing the angle of attack does not change the position of the center of pressure. One can decide if the pitch moment can disturb the stability of the train by calculating the coefficient of pitch moment. There are three cases

- Case 1:If Cm>0 in this case the train is unstable
- Case 2:If Cm <0 in this case the train is stable
- Case 3: If Cm=0 this case is ideal case in which the aerodynamic center is the same as the center of gravity.

From the results below all cases under the speed of 120km/hr fails in case 2 and also at a speed of 300km/hr when the braking plate is at an angle of 75^0 and 90^0 the results fail into case 1. The pitch moment convergence story is shown below. In all cases after the 50^{th} iteration the result diverges to one point.

4.2. Static pressure

The static pressure is high at the nose of the train body and also at the braking plate area. The highest static pressure was found at a speed of 300km/hr and at an arrangement of 90^0. At this case the maximum pressure is 3.93 Kpa. The train body can resist the given pressure perfectly.

4.2.1. At speed of 120km/hr

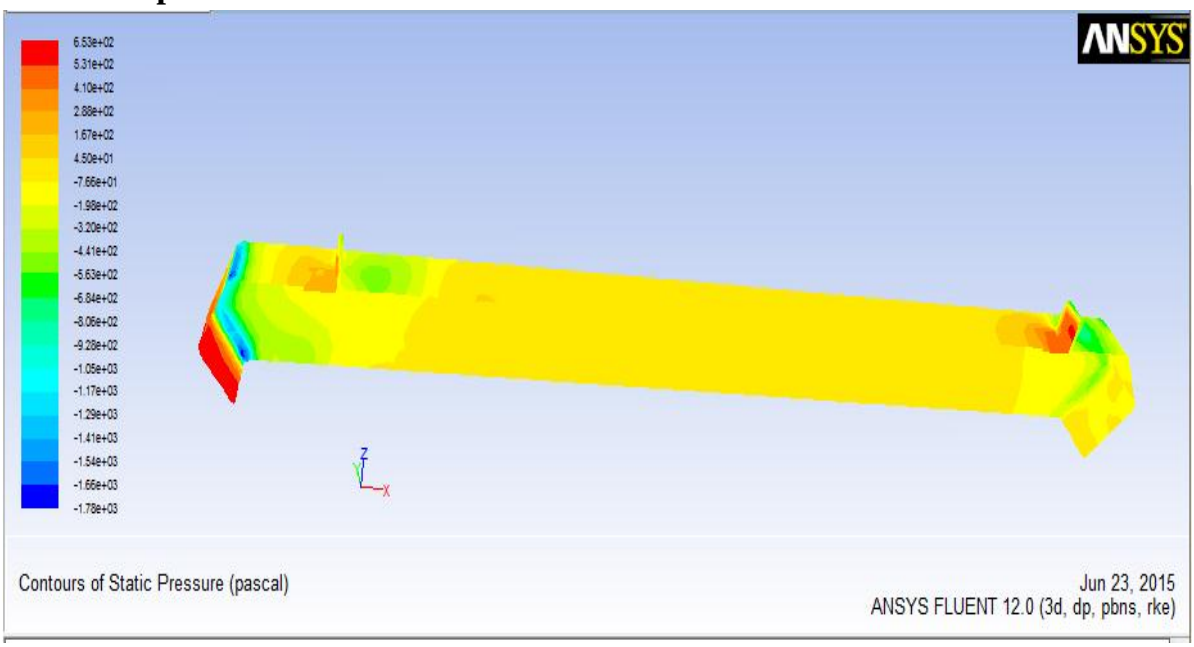

Figure 18: contours of static pressure at 90^0

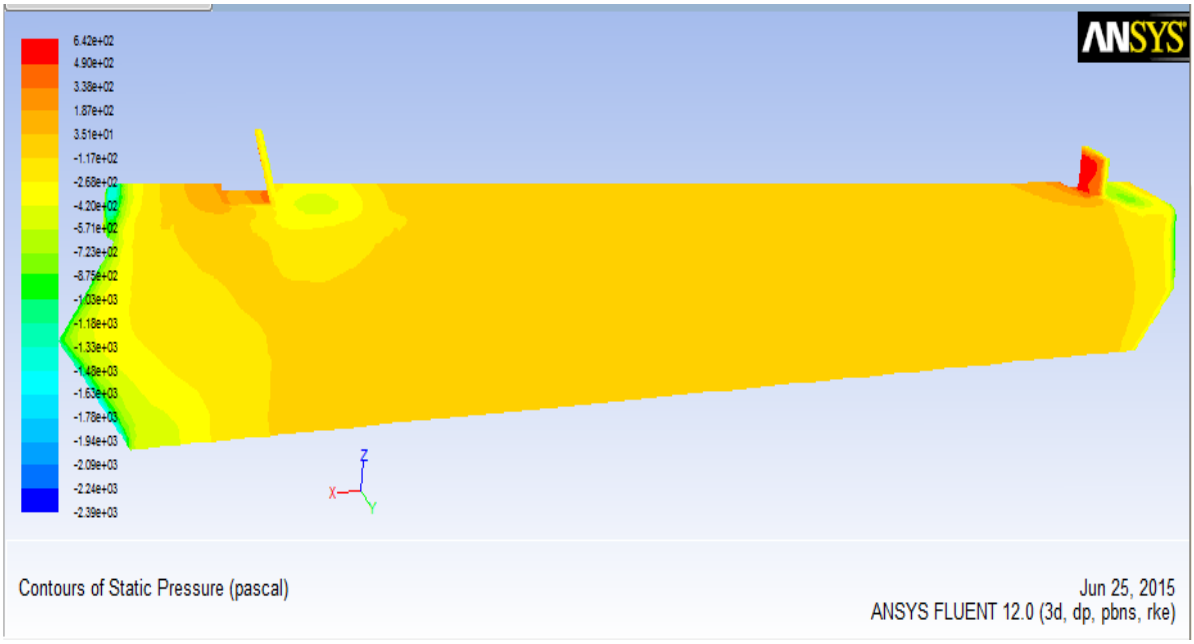

Figure 19: contours of static pressure at 75^0

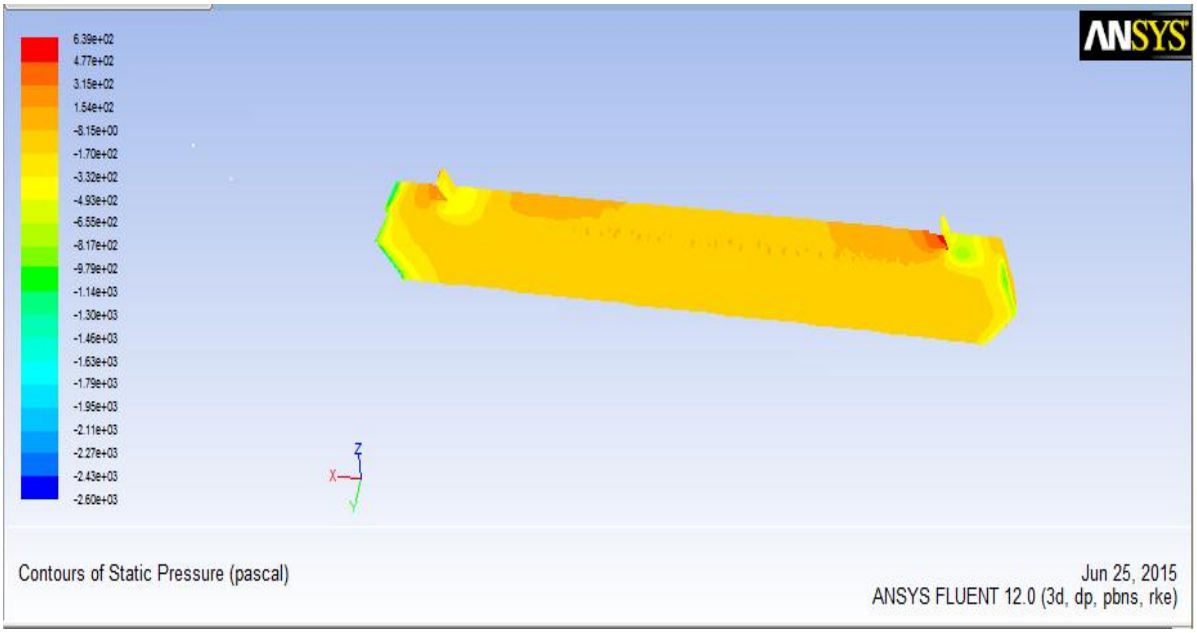

Figure 20: contours of static pressure at 60^0

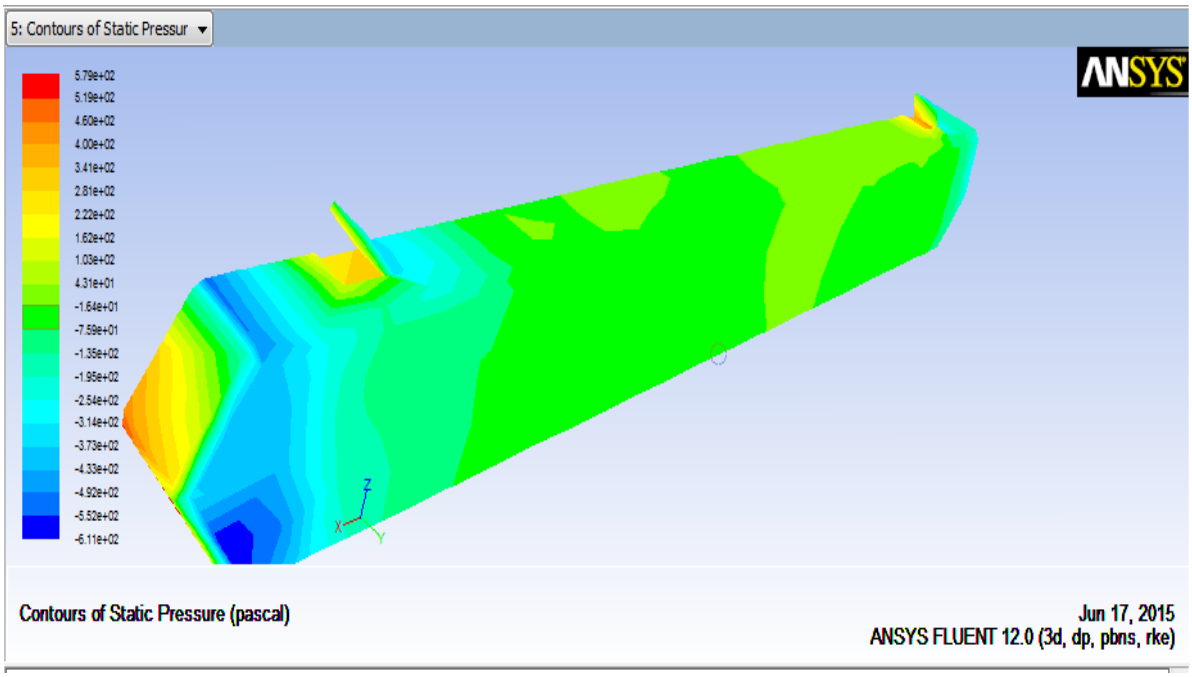

Figure 21: contours of static pressure at 45^0

4.2.2. at speed of 300km/hr

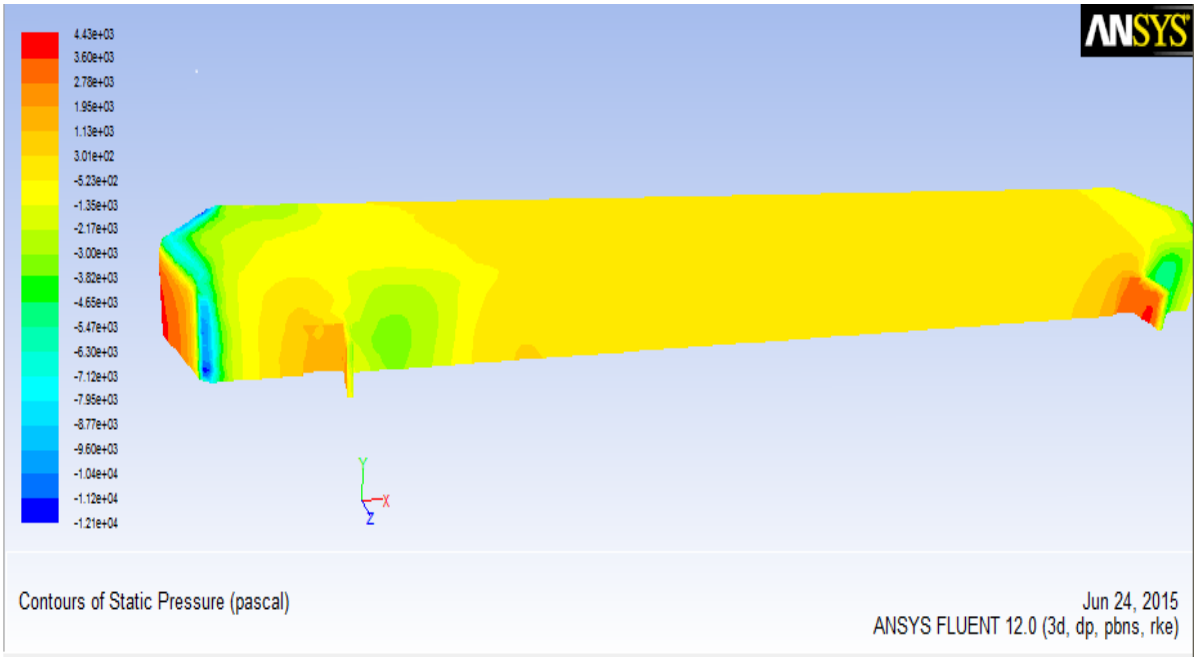

Figure 22: contours of static pressure at 90^0

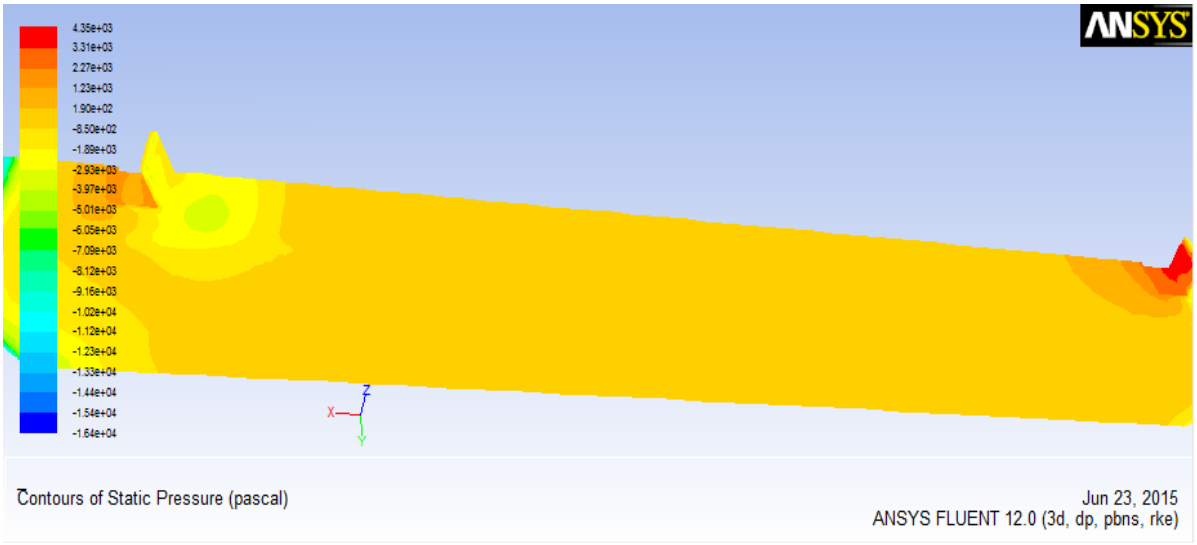

Figure 23: contours of static pressure at 75^0

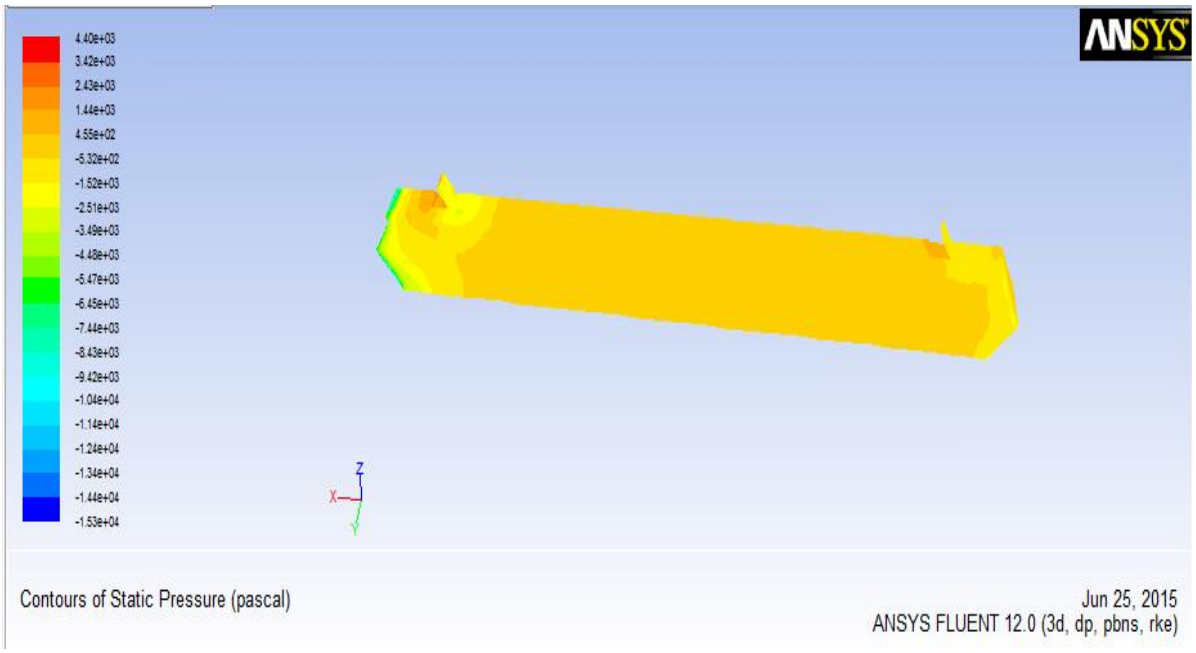

Figure 24: contours of static pressure at 60^0

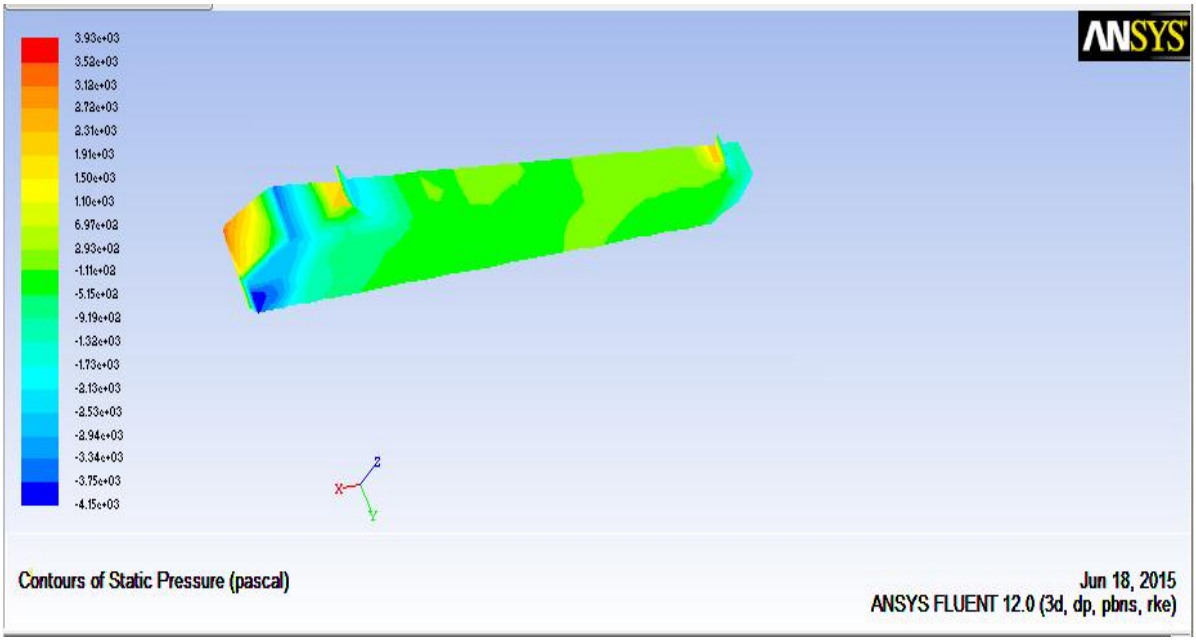

Figure 25: contours of static pressure at 45^0

4.3. Dynamic pressure

Dynamic pressure is the component of fluid pressure that represents fluid kinetic energy (i.e. motion). Dynamic pressure is minimum at the nose of the train and at the aerodynamic plates as air flow would be restricted. Dynamic pressure is high at the front edge of the train at the speed of the flow maximum at this point.

4.3.1. At speed of 120km/hr

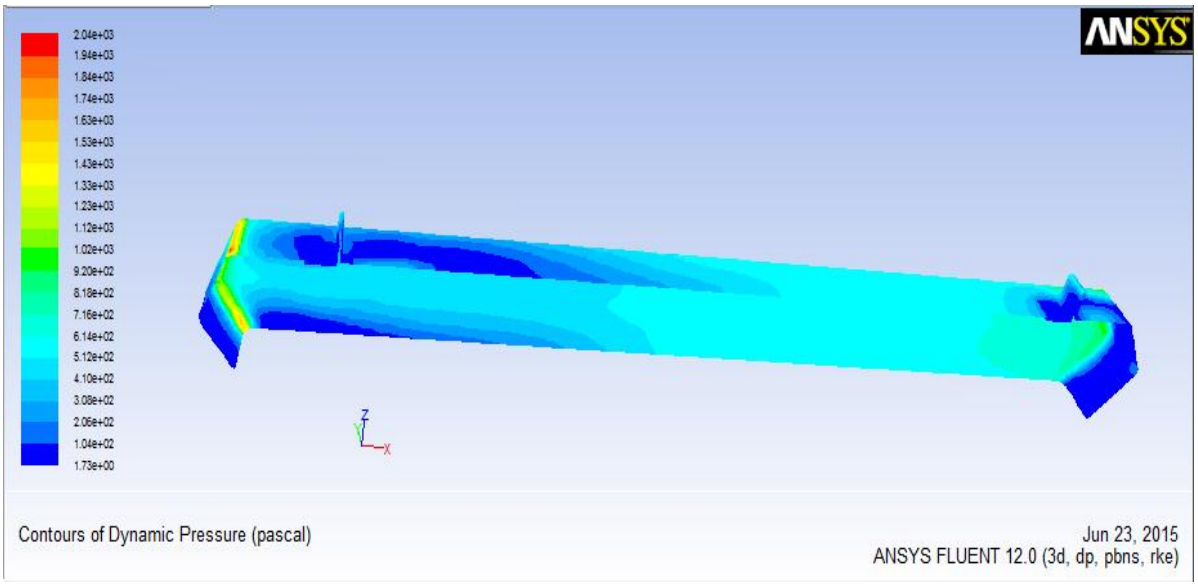

Figure 26: contours of dynamic pressure at 90^0

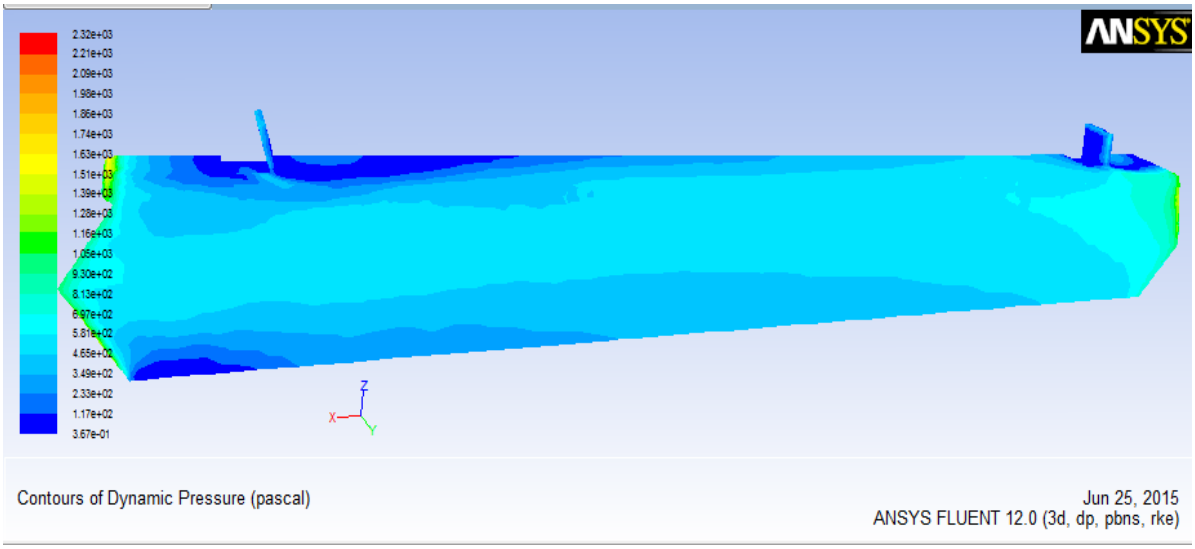

Figure 27: contours of static pressure at 75^0

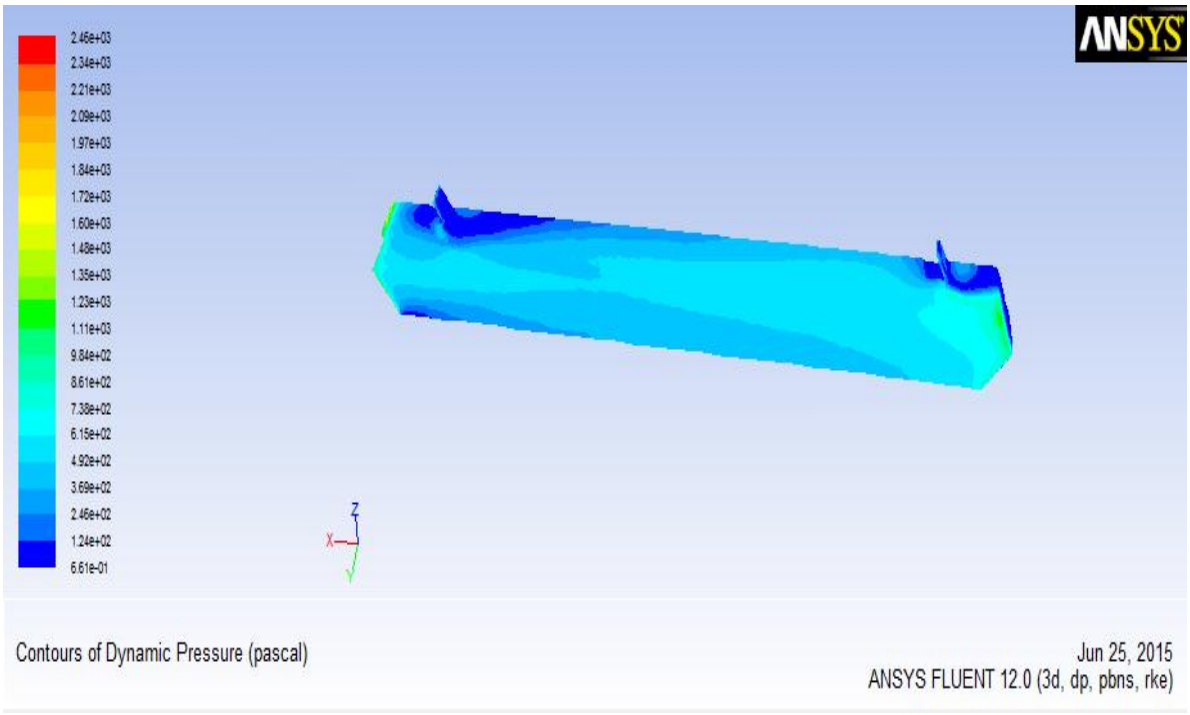

Figure 28: contours of static pressure at 60^0

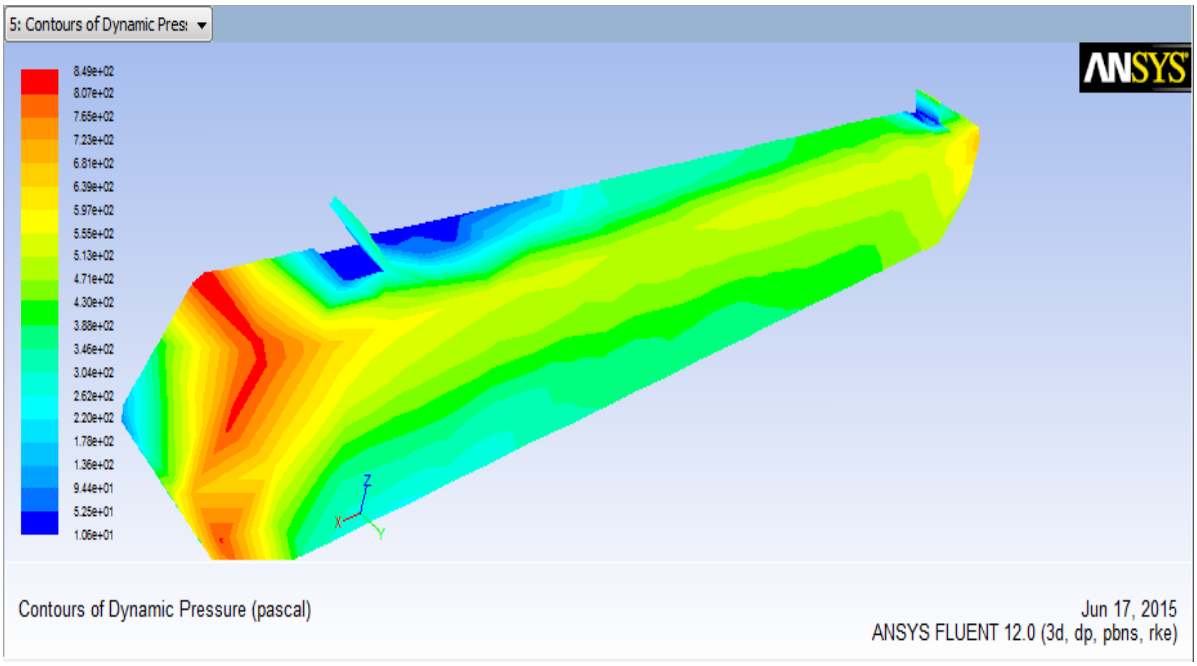

Figure 29: contours of static pressure at 45^0

4.3.2. at speed of 300km/hr

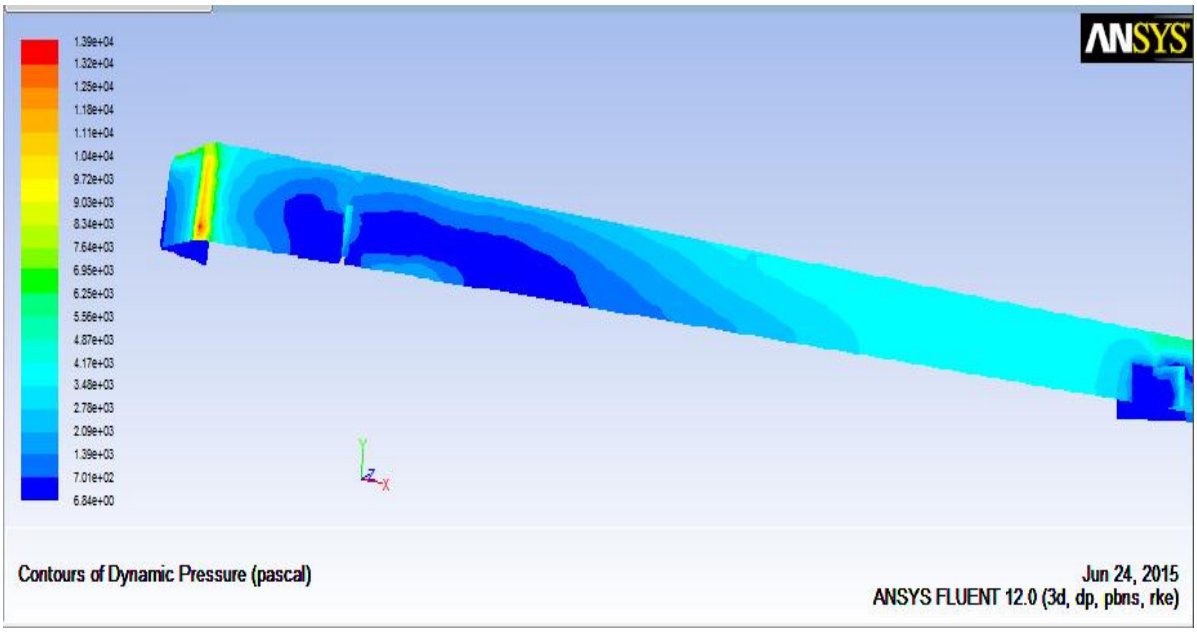

Figure 30: contours of static pressure at 90^0

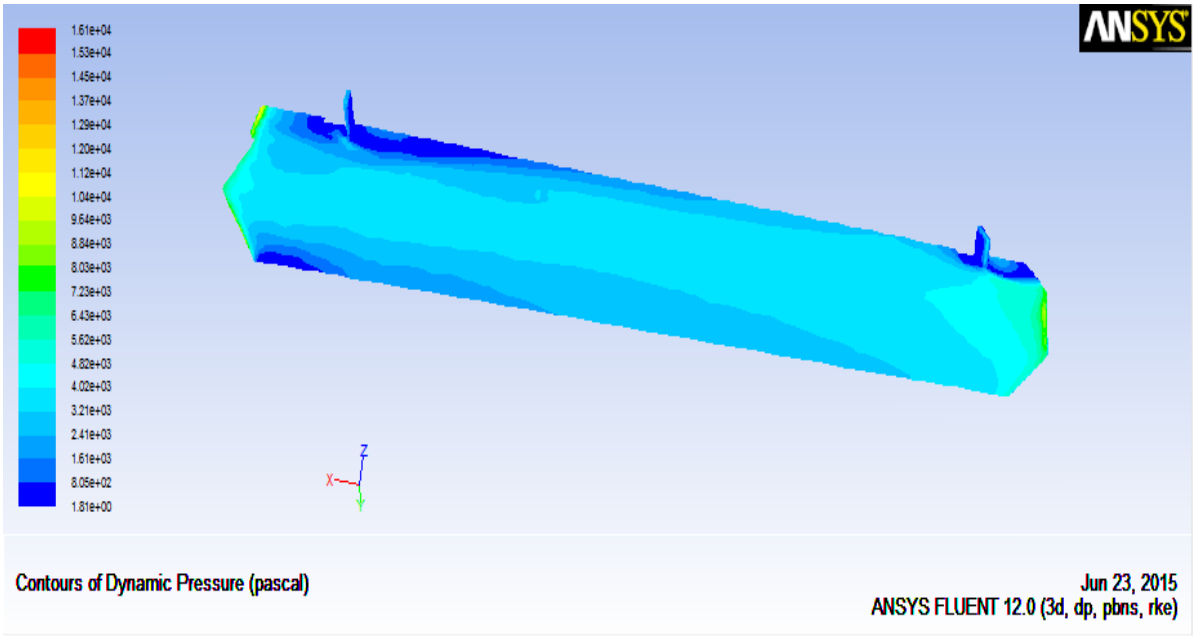

Figure 31: contours of static pressure at 75^0

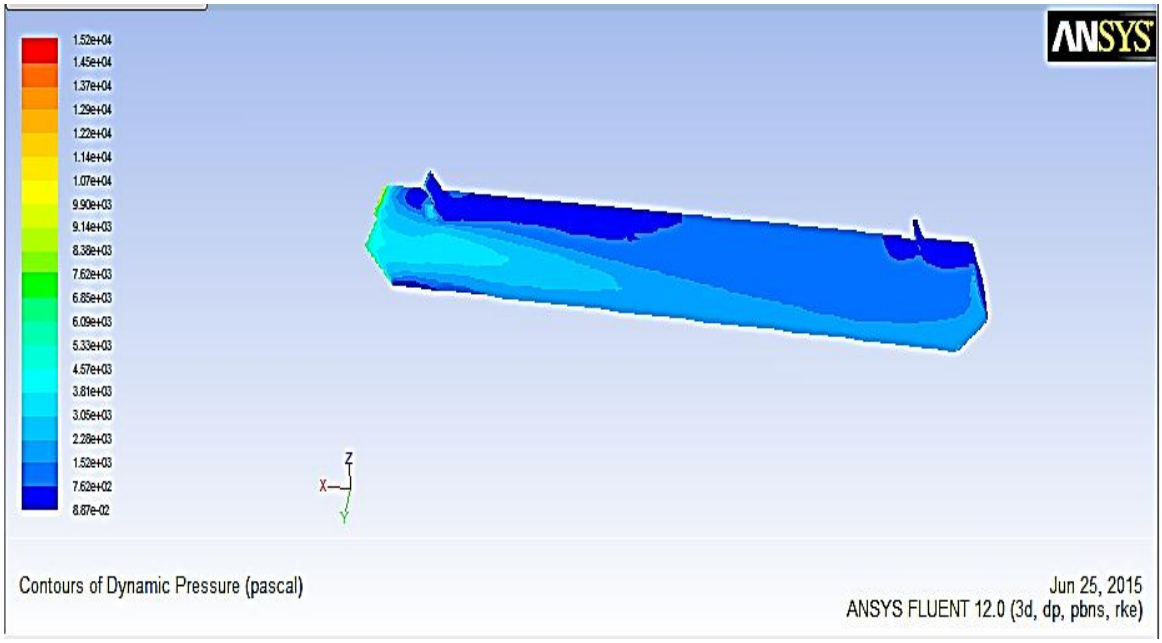

Figure 32: contours of static pressure at 60^0

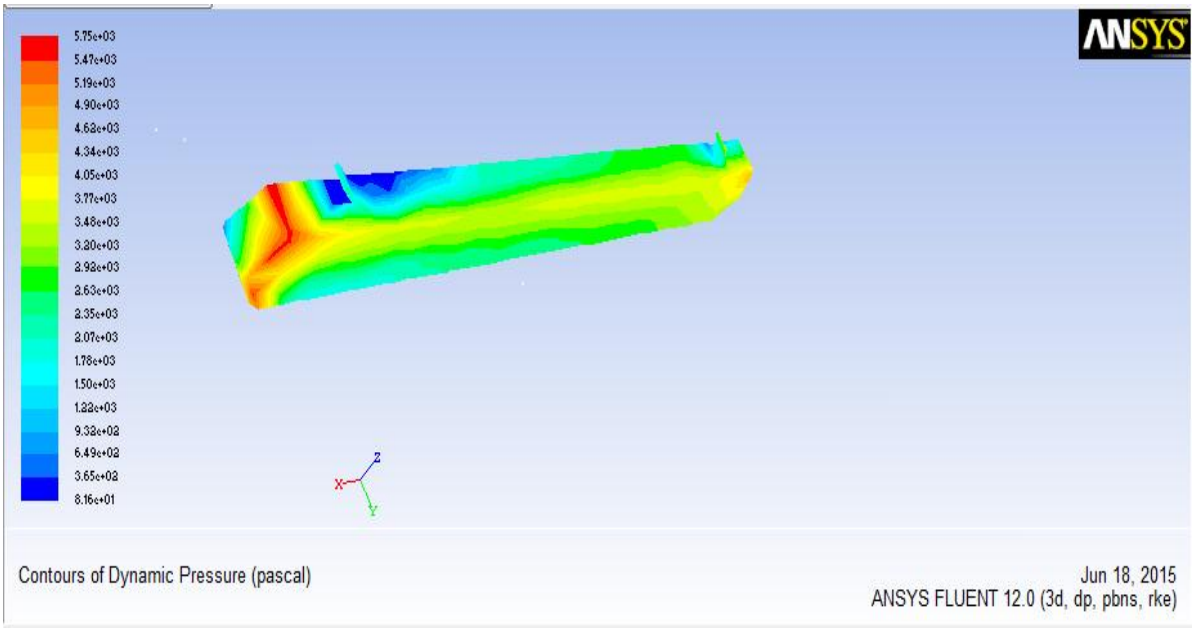

Figure 33: contours of static pressure at 45^0

4.5. Discussion

From the above results displayed it can be separated into four basic results each one will be addressed below.

The moment coefficient is directly related to the moment developed due to the drag force .and also the moment coefficient and the lift coefficients are related directly to the drag and area. This means the greater the moment coefficient the greater the moment. When the train is travelling at a speed of 120km/hr, the iterations were smooth. The values did diverge after 50th iteration .At a speed of 300km/hr at the 19th data it showed a different result but through iteration it became smooth. If this was the final step further iteration was going to be needed.

The static pressure shows a greater quantity at angle of 90 and at a speed of 300km/hr. comparing it to the value from speed of 45 degree this shows a greater change. In the results presented above the result is divided into two speeds which results in major changes. In each speed due to the braking plate angle there are different results let's look at the maximum pressure difference shown below.

Table 1: Results summary

Angle plate	120km/hr				300km/hr			
	Cl	Cm	Cd	pressure(pa)	Cl	Cm	Cd	pressure(pa)
45	0.1034	0.285	0.351	732	0.167	0.526	0.496	4400
60	0.1143	0.304	0.474	718	0.18	0.833	0.589	4480
75	0.1233	0.428	0.576	722	0.272	1.208	0.753	4410
90	0.1521	0.534	0.712	644	0.251	2.36	0.855	3930

4.6. Validation of the FE Model Result

4.6.1. Validation of drag force

The drag force needed to brake the train should be equal or greater than the required braking force. The braking force needed to brake the locomotive is calculated by using the required deceleration. The required deceleration becomes -0.68m/s^2.The calculated brake force is done by taking the weight of the locomotive to be 25t. As a result the calculated braking force becomes 17KN.The founded drag forces for each arrangement at a speed of 120km/hr is shown below

Table 2: Drag force at different arrangement

	Drag force
At 90^0	17.19KN
At 75^0	10.23KN
At 60^0	6.139KN
At 45^0	4.139KN

From the results above the arrangement that can fulfill the required brake force is when the braking plate is arranged at an angle of 90^0.

4.6.2. Validation of the pressure between crossings trains both with braking plate

The specific case which is at arrangement of 90^0 and at a speed of 120km/hr is considered here. This is because the braking force is applicable at an angle of 90^0 and the main idea of this paper is to see the application at a speed of 120km/hr. At this analysis two trains crossing each other both with braking plates were discussed. Both trains are with the same dimension and same speed at a distance of 5m from each other. The static pressure from the trains crossing is shown below

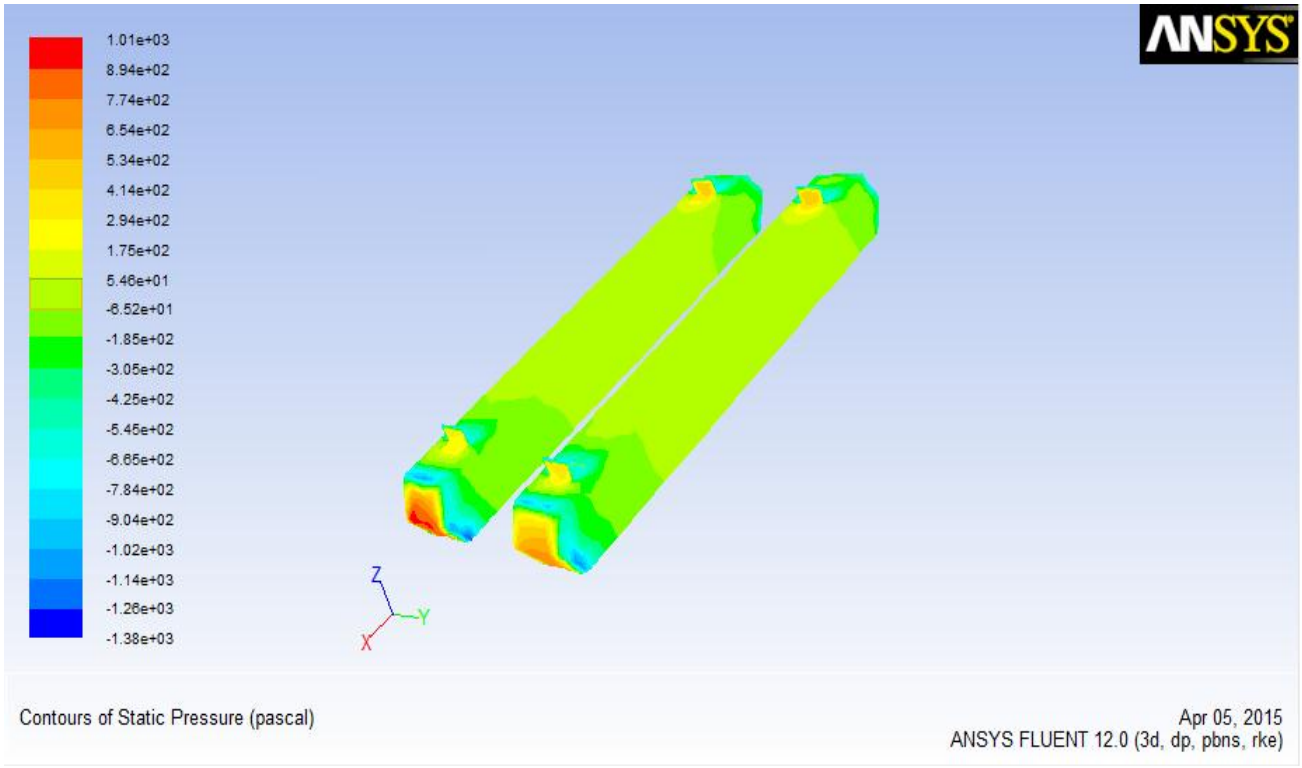

Figure 34: Contours of static pressure during crossing

The pressure change from the figure is 2.39kpa. The glass of the train windows can endure 8.28 kPa , as glass is pasted to the windows, and it will not impact the safety when the track space is 5m or more.

CHAPTER FIVE

5. CONCLUSION, RECOMMENDATION AND FUTURE WORK

5.1. Conclusion

From the above results it can be concluded that

- When two trains with aerodynamic braking pass by each other, the highest crossing air pressure is 2.39 kPa.
- When the braking plate is assembled at different angles on the vehicle body the change which is achieved on the total pressure is not as much different as expected the value varies 5-10% of the braking pressure only
- When comparing between the two velocities 300km/hr clearly brings with high pressure. The difference is greater than 2 times the pressure at 120km/hr this shows that as the speed gets higher the pressure increases but note that the moment should be taken into greater consideration. At 120km/hr the pressure is comparatively low and it shows little moment coefficient resulting in approximately no moment effect trying to rotate and pull out the locomotive from the rail.
- The drag force was increased when adding the braking plate area which is widely usable especially in emergency brake.
- As the braking plate area is increased the pressure also increases.

5.2. Recommendation

From this research the recommendations are as follows

- When using aerodynamic brakes it is more effective to use them at very high speeds.
- At the running speed of mainline that is 120km/hr this type of brake can be used without any doubt about the moment and noise effects but as the speed increases it needs a lot of considerations.

5.3. **Future work**

During this work there was the following future works of which is not completed by shortage of time at this paper

- The comparison with brake disc.
- The actuating mechanism was not discussed.

Bibliography

[1]. Anderson J.D Fundamentals of aerodynamics [Book]. - [s.l.] : McGraw-Hill, 1996.

[2]. Department Equipment Supply and Technical Services Rolling Stocks Specification.

[3]. Ganguli Surojit Numerical computation of fluid flow [Journal]. - Delhi : [s.n.].

[4]. Histor of rail transport-wikipedia the free encyclopedia [Online].http://www.wikipedia.com.

[5]. Hong-qi Tian 'Formation mechanism of aerodynamic drag of high-speed train and some reduction measures'. [Journal]. - China, : Central South University, Changsha 410075, , 2009.

[6]. Ivana Vasović Mirko Maksimović Mirjana Puharić,Dušan Matić& Suzana Linić Analysis of Aerodynamic Brakes in High -speed Trains [Journal]. - 2011. - Vol. vol 61..

[7]. Meng-ling WU† Yang-yong ZHU, Chun TIAN, Wei-wei FEI Influence of aerodynamic braking on the pressure wave of a crossing high-speed train [Journal]. - china : [s.n.], 2009.

[8]. O.Lewis Aerodynamoc anlysis of a 2-man bobsleigh [Book]. - [s.l.] : Delft University of technology, 2006.

[9]. rail transport in ethiopia [Online]. - http://www.wikipedia.com.

[10]. Ristic Slavica Determination of Braking Force on the [Journal].

[11]. Roman Momtchil Petkov and Mario CFD Training Manual [Book]. - 2011 : University of Connecticut.

[12]. S.Childress M.Ghil and Topics in geophysical fluid dynamics [Journal]. - New york : [s.n.], 1987. - applied mathimatical sciences : Vol. 60.

[13]. sadrey M.and VDM Verlag Dr.Muller Drag coefficient,2009 [Journal]. - 2009.

[14].structural analysis of aerodynamic brakes in high -speed trains [Journal]. - 2011.

[15]. T. Nathaniel Ethiopian Adventure [Journal]. - 2005. - Vol. 127.

[16]. Uchida Izumi Hasegawa and Siego braking systems [Journal]. - [s.l.] : Technology.

[17]. ZhuoJun Luo1 Jianyong Zuo1*, Liguo Zhan2 Simulation of Hydraulic system with AMESim for Aerodynamic Brake of high speed Train [Journal]. - china : Tongji University.